ARKIV FÖR KEMI

UTGIVET AV

KUNGL. SVENSKA VETENSKAPSAKADEMIEN

Band 9 nr 44

R. St. John Manley

Properties of ethyl hydroxyethyl cellulose molecules in solution

---

ALMQVIST & WIKSELL / STOCKHOLM

Uppsala 1956

R. UNIV.
BIBLIOTHEEK
LEIDEN

Properties of Ethyl Hydroxyethyl Cellulose Molecules in Solution

INAUGURAL DISSERTATION

BY

R. ST. JOHN MANLEY
PH., D., MC GILL UNIVERSITY, CANADA
FIL. LIC., VÄRML.

BY DUE PERMISSION OF THE PHILOSOPHICAL FACULTY
OF THE UNIVERSITY OF UPPSALA,
TO BE PUBLICLY DISCUSSED IN THE LECTURE HALL
OF THE INSTITUTE OF CHEMISTRY,
MAY 25, 1956, AT 10 A.M.,
FOR THE DEGREE OF 'FILOSOFIE DOKTOR'

UPPSALA 1956
ALMQVIST & WIKSELLS BOKTRYCKERI AB

R. UNIV.
BIBLIOTHEEK
LEIDEN

ARKIV FÖR KEMI Band 9 nr 44

Communicated 11 April 1956 by The Svedberg and Arne Fredga

Properties of ethyl hydroxyethyl cellulose molecules in solution

By R. St. John Manley

With 28 figures in the text

Contents

Page

Preface 519
Introduction 520
Part 1. Experimental procedures and results
1. Fractionation of ethyl hydroxyethyl cellulose 523
2. Preparation of solutions 525
3. Viscosity 526
4. Osmotic pressure 532
5. Specific refractive index increment 536
6. Sedimentation 537
7. Diffusion 543
8. Partial specific volume 548
9. Molecular size and shape from sedimentation–diffusion 548
10. Sedimentation equilibrium 551
11. Light scattering 554
Part 2. General discussion
1. Molecular weights and polydispersity of the fractions 561
2. Molecular weight dependence of $[\eta]$, s and D 568
3. Relation of hydrodynamic behavior to molecular configuration 570
Summary 578
References 579

Preface

The work to be described in the following pages has been carried out at the Institute of Physical Chemistry of the University of Uppsala, Sweden, under tenure of a post doctoral research fellowship from the National Research Council of Canada. I am indebted to them for providing me with this opportunity of broadening my research experience.

I wish to express my deep gratitude to the director of the Institute, Professor Stig Claesson, for his great interest in the work, for his kindly advice and encouragement and for placing the excellent facilities of the Institute at my disposal.

My sincere appreciation is also due to Dr. Ingvar Jullander for his unfailing interest and cooperation and for many valuable discussions.

The routine calculations in connection with the sedimentation and diffusion experiments have been performed by the staff of the calculating department at the

Institute. I wish herewith to express my warmest thanks to these and other members, past and present, of the Institute who on numerous occasions have given me the benefit of their judgement or of their aid and who have constantly provided the moral support of friendship and interest in this work.

Finally I wish to acknowledge my indebtness to Mo och Domsjö AB., Sweden for the many ways in which they have aided this investigation.

Introduction

Cellulose is one of the most abundant of all naturally occurring organic substances and has very great importance both technically and economically. From a purely scientific viewpoint the study of cellulose provides many research problems; during recent decades cellulose and its derivatives have been the subjects of intense investigation and many important questions have been answered although great difficulties, both of an experimental and theoretical nature have been encountered. An extensive survey of our present knowledge in this field has been given by Ott (1). In the following, a short orientation is given as an introduction to the present work.

The chemical structure of cellulose is now well established. The cellulose molecule can be considered as resulting from a 1–4 polycondensation of beta-glucose to form a chain molecule composed of a large number of six membered rings, normally called glucose residues. The number of glucose residues in a cellulose molecule may be of the order of several thousand. Within a cellulose fiber the chain molecules are bound laterally to another by hydrogen bonds in such a way as to form crystallites (small crystalline areas) separated by amorphous regions. The reactivity of the cellulose in the amorphous regions is greater than in the crystallites. Although the cellulose molecule has been widely investigated no definite conclusion can be drawn as to its size. Existing methods for the determination of the degree of polymerisation have given results varying from about 200 for viscose silk to 5000 for native cotton cellulose. All the known methods of dissolving cellulose are assumed to cause depolymerisation to a greater or lesser degree; cellulose is known to be polymolecular in solution and possibly is so also in its native state.

In solution, molecules of cellulose and its derivatives possess an unbranched thread-like form. Depending upon the solvent, the temperature and the degree of polymerization a given cellulose molecule may assume different configurations ranging from that of a completely randomly coiled chain to that of an almost linear rod. However, in recent years it has been shown that, compared with most other polymers, the molecules of cellulose and its derivatives tend to be relatively rigid in solution.

From an organic chemical point of view cellulose can be regarded as an alcohol; it undergoes some of the reactions characteristic of this group of substances—in particular ether and ester formation. The esters are by far the most important and well known of the cellulose derivatives. The best known representatives of this class are cellulose nitrate and cellulose acetate, both of which were discovered already around the middle of the nineteenth century.

The ethers of cellulose are considerably more recent. Broadly speaking, two types may be distinguished: cellulose ethers soluble in organic media and cellulose ethers soluble in water and alkali. The present study is concerned with a cellulose ether and we therefore restrict our attention to this class.

The etherification process generally consists of the preparation of alkali cellulose by interaction of cellulose with a base and solvating agent and the reaction of the alkali cellulose with an etherifying agent (e.g. an alkyl halide). Byproducts of the reaction are removed by washing with methanol–water or ethanol–water solutions or in some cases with boiling water. After drying, the product is obtained in a flaky or powdery form of white or yellow-white colour.

In all cases there is no certainty as to the position of the substituents in the anhydroglucose units. This problem has been discussed by Timell (2). Equally scant is our knowledge of the distribution of substituents along the chain.

The properties of cellulose ethers vary with the degree of substitution, with the degree of polymerization and the nature of the substituent. The solubility of cellulose ethers is largely controlled by the degree of substitution. Cellulose itself is not water soluble, despite the fact that it contains a larger number of hydroxyl groups. This is due to the fact that the molecules are strongly bound to one another by hydrogen bonds. In alkali, cellulose swells but does not dissolve. The partial replacement of the hydroxyl groups by more bulky substituents serves to break up the superstructure, thereby weakening the hydrogen bonds so that solubility in water becomes possible. With increasing degree of substitution a given ether will be soluble first in alkali, then in water and finally in organic solvents.

The solubility of cellulose ethers is also influenced by the distribution of the substituents. If the groups are uniformly distributed along the chain, better solubility will be observed than if complete substitution occurs in some sections of the chain alternating with sections of no substitution. In regions where there is no substitution, packing similar to cellulose itself will exist, provided the sections are long enough, with the result that such sections will resist solution and hence interfere with complete solubility.

The degree of polymerization of cellulose ethers can also be varied within wide limits. It depends partly on the type of cellulose used as the starting material and partly on the temperature of reaction. The nature of the substituent also plays an important role in determining the properties of the ether. One may distinguish between ionic and non-ionic ethers. The best known representative of the former group is carboxymethyl cellulose. Members of the latter class contain methyl, ethyl or hydroxyethyl groups either singly or in various combinations.

A characteristic of all non-ionic water soluble cellulose derivatives is that they cause a very strong decrease in the surface tension of water and they are therefore used as emulsifiers. The marked tendency of the solutions to foam makes experiments somewhat more difficult. Finally it may be mentioned that water soluble cellulose ethers which contain ethyl or methyl groups are soluble only in cold water. On warming, flocculation or gelation occurs but on cooling, the ether again becomes soluble. A description of the preparation and properties of water soluble cellulose ethers has been given by Jullander (3).

In comparison with cellulose esters very few studies have been made of the solution properties of cellulose ethers. The molecular weight of carefully fractionated samples of water-soluble methyl cellulose was determined by Signer and coworkers (4, 5) and Polson (6) from sedimentation equilibrium, viscosity and diffusion. Osmotic pressure and viscosity measurements on similar methyl celluloses have been made by Staudinger and coworkers (7). More recently Jullander (8) has described some of the properties of ethyl hydroxyethyl cellulose.

The effect of salt on solutions of these ethers has been studied by a number of

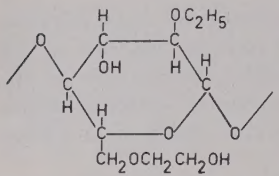

Fig. 1. Schematic structural formula of the repeating unit in ethyl hydroxyethyl cellulose.

authors (9–13). The addition of salt causes dehydration of the cellulose chains and at sufficiently high salt concentrations flocculation or gelation occurs. The ability of various salts to cause flocculation generally follows the Hofmeister series.

As has been emphasised by Jullander (8), water soluble cellulose derivatives never dissolve completely. In addition to the molecularly dispersed cellulose chains a solution contains molecular aggregates of submicroscopic size, gel particles and undissolved fibres. This fact has seldom been taken into consideration in physico-chemical investigations of the properties of water soluble cellulose derivatives and may certainly be expected to lead to difficulties. The same phenomena is observed in solutions of other polymers, for example rubber both of natural and synthetic origin and viscose. In the former case it is due to cross-linking and in the latter to the different reactivity of the crystalline and amorphous regions in the cellulose.

This paper gives an account of an investigation of a non-ionic water soluble cellulose derivative namely ethyl hydroxyethyl cellulose. The schematic structural formula is shown in Fig. 1. It is a mixed ether prepared by the reaction of alkali cellulose with a mixture of ethylene oxide and ethyl chloride in an autoclave. Details of the preparation have been given by Sönnerskog (12). It is manufactured commercially by Mo och Domsjö AB, Sweden, and is marketed under the trade name of *Modocoll*. Its properties, which are similar to those of other cellulose ethers, have been described by Jullander (8, cf. also Sönnerskog, 12). One property deserves emphasis at this point. When an aqueous solution of ethyl hydroxyethyl cellulose prepared at room temperature is cooled to about 5°C, the viscosity increases irreversibly and the solution becomes considerably clearer. This is probably partly due to increased molecular solvation at low temperatures and partly also to the low temperature dissolution of fibers which are inhomogeneously etherified or have a very resistant structure (8). On heating, the viscosity decreases and gelation begins at a temperature of about 50°C.

Ethyl hydroxyethyl cellulose is a relatively new polymer whose physico-chemical properties have not been previously investigated. In some respects the substituent groups have quite different characteristics, for example, the ethyl group is hydrophobic, while the hydroxyethyl group is hydrophilic. It was of interest to see whether this would confer any unique properties upon the behavior of the molecules in solution. Furthermore, because of the fact that the polymer is water soluble and non-ionic its thorough study might be expected to provide background information for the theoretical treatment of the more complicated polyelectrolyte systems based upon the cellulose skeleton.

In order to obtain as complete a characterization as possible, a wide variety of methods has been used. The goal was not to make precision measurements of molecular parameters, but rather to try to get a broad overall view of the molecular behavior in solution. Studies have been made of the viscosity, sedimentation, diffusion, osmotic pressure and light scattering of various samples prepared by

fractionation. In this way a series of molecular weight averages is obtained and the many methods used therefore serve not only as a mutual check on the reliability of the results but also as a means of estimating the breadth of the molecular distributions in the samples. As will be seen later this latter point is of considerable importance in evaluating the data. Furthermore, the relation between the various molecular constants, intrinsic viscosity, sedimentation and diffusion coefficients and the molecular weights give information about the shape of the molecules.

The aim of the work has also been to determine the manner in which the data obtained fit into the frame of current theories on the behavior of flexible linear macromolecules in dilute solution and to interrelate some of the results in terms of fundamental molecular parameters.

The work is presented in two parts, the first of which deals with various aspects of the experimental work. Whenever possible, comparisons are drawn to corresponding data available in the literature. The second part is devoted to a general discussion of the experimental results and their evaluation in the light of current theory.

Part I

Experimental procedures and results

(1) Fractionation of ethyl hydroxyethyl cellulose

The material used was a commercial sample (Modocoll E 600)[1] and was used without further purification. Analytical data are given in Table 1.

As is well known, the fractionation of high polymers largely depends on the very small decrease in solubility with increase in molecular weight in a given polymer

Table 1. Fractionation of ethyl hydroxyethyl cellulose.

Fraction No.	wt. of fraction g	Extractant acetone–H_2O wt. %	$[\eta]_{25}$ dl/g	Ethoxyl %	Ethoxyl + hydroxyethyl %	NaCl %
Original	—	—	6.2	18.0	33.3	0.9
1	18.6	80	1.30	21.8	25.6	3.2
2	16.9	65	2.60	19.6	31.5	0.1
3	24.6	50	3.49	18.5	31.1	0.1
4	26.4	45	4.20	18.3	31.5	0.1
5	19.5	39	4.70	17.9	29.1	0.3
6	22.0	34	5.70	17.8	28.4	0.2
7	24.4	25	6.75	17.5	30.0	—
8 A	13.9	20	7.90	17.1	29.9	—
8 B	14.3	20	7.00	17.1	32.5	—
9	31.3	15	8.70	17.4	29.5	—
10	30.7	10	8.90	17.6	29.9	0.1
11	15.7	5	8.90	17,6	30.0	0.3
12	20.1	0	9.10	18.0	29.6	0.1

[1] Manufactured by Mo och Domsjö AB, Sweden.

series. Two methods have generally been used, fractional precipitation from a dilute solution and fractional extraction.

In the case of cellulose derivatives the solubility depends not only on the degree of polymerization but also on the chemical composition. However, a proper choice of solvent–non-solvent systems may result in fractionation being effected mainly according to one of these factors.

In the case of the material under investigation the problem was complicated by the fact it is only soluble in water. This had the effect of severly limiting the choice of non-solvents for fractional precipitation. Methanol, ethanol, propanol, dioxane, acetone and solutions of sodium chloride and sodium sulphate proved to be inefficient and great difficulties were experienced in isolating the precipitated phase which remained dispersed even after prolonged centrifugation at about 2000 r.p.m.

These difficulties were surmounted by the use of a fractional solution method. The solid material retained in finely divided form was extracted isothermally (20°C) with acetone-water mixtures of increasing solvent power, the polymers of lowest molecular weight being extracted first from the sample. So as to ensure that a sufficient quantity of each fraction would be available for the large number of experiments invisaged, 500 g of starting material was used. In order to get maximum efficiency of separation large volumes of extractant (15–20 litres) were used and the extraction was allowed to continue until equilibrium was established. This condition was considered to exist when two or three successive gravimetric analyses (evaporation to constant weight of an aliquot) taken over intervals of twenty-four hours showed a constant amount of material in solution. The establishment of this equilibrium took rather a long time varying from three days for the low molecular weight fractions to approximately two weeks for fractions of higher degree of polymerization.

After the attainment of equilibrium the solution was separated by centrifugation and the residue treated with an extractant containing less acetone. At the end of the fractionation there remained an insoluble residue probably consisting of partially etherified fibers.

With the exception of the first fraction, which was concentrated under vacuum at 30°C and then freeze-dried, the polymer in the acetone-water solution was coagulated by the addition of excess acetone (approx. 4 pts. acetone to 1 pt. soln.). The polymer settled spontaneously and the supernatant liquid was decanted. The material was then dried at 35°C under vacuum after exhaustive washing with ethanol followed by benzene. Material dried under similar conditions directly from water produced a hard horny mass which was difficult if not impossible to redissolve.

Twelve fractions were thus obtained, each weighing about 25 g, and were designated M1–M12, 12 being that of highest degree of polymerization. The average degree of substitution (see Fig. 1) was 0.56 with respect to ethoxyl (OC_2H_5) and 0.84 with respect to ethylene oxide (OC_2H_4) and varied slightly from fraction to fraction. The corresponding average base molar weight is 210.

An interesting fact which perhaps deserves mention is that as the fractionation proceeded, increasing difficulty was experienced in effecting quantitative coagulation of the polymer in solution. Generally there was about 90 per cent recovery, the remainder of the material being dispersed in the liquid phase regardless of how great an excess of acetone was added. Thus in fraction 8 only 50 per cent of the material was recovered by coagulation. However, it was discovered thereafter that the remainder of the material in the supernatant phase could be quantitatively precipitated by the addition of a very small quantity of sodium chloride solution

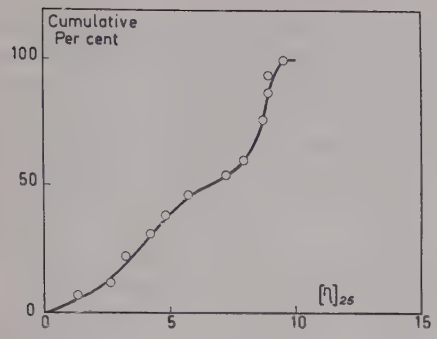

Fig. 2.

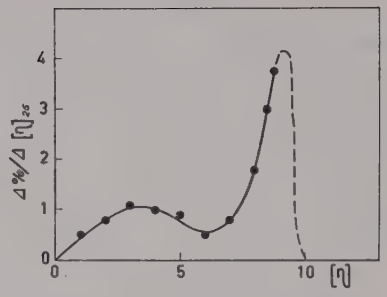

Fig. 3.

Fig. 2. Integral distribution curve for the unfractionated sample of ethyl hydroxyethyl cellulose. The curve is constructed from the weights and intrinsic viscosities of the fractions.
Fig. 3. Differential distribution curve for the initial sample of ethyl hydroxyethyl cellulose as obtained by graphical differentiation of the integral curve (Fig. 2).

(1 c.c. 0.5 per cent NaCl solution per 20 litres of polymer solution). The effect seems to be connected with the fact that with each successive extraction more and more of the salt present in the original material was washed out, thus making it possible for a part of the polymer to become colloidally dispersed. The degree of polymerization and degree of substitution of the two parts of the fraction were quite different.

The ethoxyl content of each fraction was determined after Lemieux and Purves (14). The material is oxidized with chromic acid solution, the ethoxyl groups being transformed into acetic acid which is distilled off and titrated. The sum of the ethoxyl and hydroxyethyl groups was determined by the modified alkoxyl group method described by Morgan (15). The hydroxyethyl content was obtained as the difference between the ethoxyl content and the total substitution. The salt content was determined by titration against silver nitrate.[1] The intrinsic viscosity of each fraction was measured with an Ubbelohde viscometer. Details of these measurements will be given later.

The results of the fractionation are shown in Table 1. It would appear that the method of fractionation lacks sensitivity in the high molecular weight range there being little or no separation between fractions 10–12. The material of low degree of polymerization is most highly substituted but within the limits of experimental error the degree of substitution is constant in the medium and high molecular weight ranges.

Molecular distribution curves for the starting material, constructed on the basis of the fractionation, are shown in Figs. 2 and 3. It is evident that the sample was extremely polydisperse.

(2) Preparation of solutions

Fractions M3, M5, M7 and M12 were selected for measurements and were used without further purification.

All measurements were made from standard solutions which were prepared as follows: To a weighed quantity of the polymer about 25 per cent of the volume of

[1] The author is indebted to Mr. O. Lagerström at the Laboratories of Mo och Domsjö AB, Sweden, for carrying out these analyses.

water needed to produce the required concentration was added as hot water (80–100°C) and the container was maintained at this temperature for about thirty minutes. Cold water (< 10°C) was then added to produce the required concentration. The addition of hot water causes swelling of the fibers thereby hastening the solution process upon the addition of cold water. This treatment had the further advantage that it helped to minimise the formation of gel around the solid particles, a phenomena frequently encountered in the dissolution of high polymers.

The dispersion thus formed was vigorously shaken for about 48 hours in a cold room at 4°C. As the viscosity of a solution depends on the lowest temperature to which it is subjected (8), all solutions were then frozen and later thawed out.

Preliminary experiments indicated that small amounts of salt could have an effect upon the viscosity behavior, a 10 per cent decrease in $[\eta]$ being obtained in the range 0–30 $\times$ 10^{-4} molar NaCl. This effect seems to be similar to that observed by Pals and Hermans (16) for aqueous solutions of polyvinylalcohol and is probably the result of ion adsorption. Accordingly all solutions were rendered salt free by passage through an ion-exchange column containing a mixed bed (Dowex 50—acid form and Amberlite IRA 400—base form). The solutions were sufficiently dilute that there were no difficulties due to clogging of the column. By measuring the viscosity of a solution, freed from salt by electrodialysis, before and after passage through a similar column it was established that there was no selective adsorption of polymer species on the resin.

The salt free solutions were cleaned by centrifugation in the large rotor of a Spinco preparative ultracentrifuge (30,000 r.p.m. for 2 hours). In all cases a small gel-like deposit was obtained. The solutions were then stored in a refrigerator at 4°C. Fresh solutions were prepared about once per month.

In all experiments concentrations were determined by evaporating a portion of the solution to constant weight at 105°C. A conversion to units of grams per 100 c.c. was made from a knowledge of the density of the solution. This method is known to be inaccurate in certain cases (17), since the film of polymer that is formed on the walls of the containing vessel may still retain an appreciable percentage of volatile material. In the present case, the fact that the heating of the solution causes precipitation means that there is no "glass" formation and the solvent is easily and completely removed by the evaporation. Constant weight was attained in 6–8 hours.

(3) Viscosity

All viscosity measurements were made with an Ubbelohde type capillary viscometer. The non-Newtonian behavior of the solutions was taken into account by constructing the viscometer with four bulbs at different heights to allow measurements at four gradients. A large reservoir (120 c.c.) was provided so that dilutions could be carried out in the instrument. In order to avoid difficulties caused by dust a capillary of relatively large radius was used. The capillary was coiled in the form of a wide smooth loop in a vertical plane. It was made of precision Hysel tubing the radius of which was determined by measuring the weight of mercury in a given length. The design of the instrument is similar to that used by several authors (cf. e.g. ref. 18). The dimensions of the instrument are given in Table 2.

The mean hydrostatic head, h_m, was calculated from the formula (19)

$$h_m = \frac{h_1 - h_2}{\ln h_1/h_2}$$

Table 2. Viscometer dimensions and constants.

Efflux bulb No.	1	2	3	4
Efflux volume (c.c.)	2.50	2.01	1.21	0.60
Mean hydrostatic head (cm) . .	28.6	23.7	14.4	6.72
Flow time for water at 25°C (sec)	152.1	146.2	140.3	155.5
Surface tension constant				
$C \times 10^4$ c.g.s. units	1.3	0.2	−1.0	−3.8
$\alpha \times 10^3$	5.912	6.143	6.392	5.741
β	0.9799	0.7620	0.4378	0.7702
β/α	163.7	124.0	68.5	−134.2

Capillary length: 30.0 cm.
Capillary radius: 0.50 mm.

where h_1 and h_2 are respectively the distances between the upper and lower mark on each bulb, and the lower end of the capillary.

The viscosity, η, may be expressed in the form:

$$\frac{\eta}{d} = \alpha (t - \beta/\alpha t), \tag{1}$$

the constants α and β being given by

$$\alpha = \pi r^4 h g / 8 V l$$
$$\beta = m V / 8 \pi l$$

where h is the mean hydrostatic head, g is the accelaration due to gravity, d is the liquid density, V is the volume of liquid delivered in time t, r is the radius of the capillary, l its length, and m is an end constant depending, among other things, on the shape of the ends of the capillary (usually taken as 1.1).

The constants α and β were determined by measuring the efflux time for water at 0, 15, 25 and 40°C. By plotting $\eta t/d$ (using values of η and d taken from the International Critical Tables) against t^2 a smooth straight line was obtained which, fitted by the method of least squares, gave α and β as the slope and intercept respectively. Values obtained for each bulb are given in Table 2. Wherever necessary the small kinetic energy correction (highest value about 0.8 per cent for solutions at 40°C) was applied using the relation

$$\frac{\eta_s}{\eta_0} = \frac{d_s t_s}{d_0 t_0} \left[1 + \frac{\beta}{\alpha} \left(\frac{1}{t_0^2} - \frac{1}{t_s^2} \right) \right] \tag{2}$$

where the subscripts s and 0 refer to solution and solvent respectively.

The mean velocity gradient $\bar{G}$ in the viscometer was calculated from the formula of Kroepelin (20)

$$\bar{G} = \frac{8V}{3\pi r^3 t}, \tag{3}$$

the symbols having the aforementioned significance. For the solutions used the values calculated covered a range 50–1000 sec^{-1}.

As previously mentioned the solutions under investigation are highly surface active and it was therefore considered necessary to investigate the possible effect of this on the viscosity measurements. As there are only relatively few discussions of such effects in the literature (21, 22, 23) the results are given in some detail. The method used resembles that described by Philippoff (23) and is based upon the following considerations.

In a capillary of radius r the capillary rise due to surface tension is given by the well-known formula $2\gamma = h\,d\,g\,r\cos\theta$, γ being the surface tension of the liquid, h the capillary rise, θ the angle of contact of the liquid with the walls of the capillary, and the other symbols have the usual significance. The surface tension causes a change in the efflux time which can be represented by the relation

$$t_{\text{obs}} = t_{\text{corr}}\, H_0 \Big/ \left(H_0 - \int_{h=H_0}^{h=H_e} \frac{2\gamma}{d\,g\,r\cos\theta}\,dr\right) \tag{4}$$

where the integral is taken over the limits from the initial (H_0) to the equilibrium height (H_e) and t_{obs} and t_{corr} are the observed and corrected efflux times respectively.

If the integral is incorporated in an apparatus constant, C, it may be readily shown that for dilute solutions

$$(\eta_r)_{\text{obs}} = (\eta_r)_{\text{corr}}\left[1 + C\left(\frac{\gamma_0}{d_0} - \frac{\gamma_s}{d_s}\right)\right] \tag{5}$$

where η_r is the relative viscosity and the subscripts have the above mentioned significance. γ_0 and γ_s are the surface tensions of solvent and solution respectively and d_0 and d_s the corresponding densities.

The value of C was determined by measuring the relative viscosities of a number of dilute solutions of sodium oleate and Teepol (a synthetic cationic detergent) and extrapolating the data for each of the four bulbs to infinite dilution.

If the surface tension is independent of concentration in the concentration interval investigated, it is clear that in the absence of disturbing factors the extrapolated value of η_r must be unity and the fact that it is not so may be attributed to surface tension effects. Measurements were made at 25°C. The results for Teepol are shown in Fig. 4. Thus, setting $(\eta_r)_{\text{corr}} = 1$ and taking $(\eta_r)_{\text{obs}}$ from Fig. 4 the magnitude of C may be calculated if the surface tensions of the solutions are known. These were measured by the capillary rise method. Over the concentration range investigated (0.1–0.4 per cent for sodium oleate and 0.5–2.0 per cent for Teepol) the surface tensions were essentially constant and the value in this range (26 and 32 dynes/cm for sodium oleate and Teepol respectively) was used to evaluate C. The values of C obtained with sodium oleate and Teepol agreed to within 1 per cent except for measuring bulb 2 where there was a 3 per cent difference. The mean values given in Table 2 were used for further calculations. The sign of the constant C indicates whether the efflux time is increased or decreased by the surface tension. These effects depend upon the relative size and shape of the meniscus in the measuring bulb and lower end of the capillary respectively; the efflux time may be increased or decreased depending upon this factor.

The surface tensions of the polymer solutions were also measured by the capillary rise method.

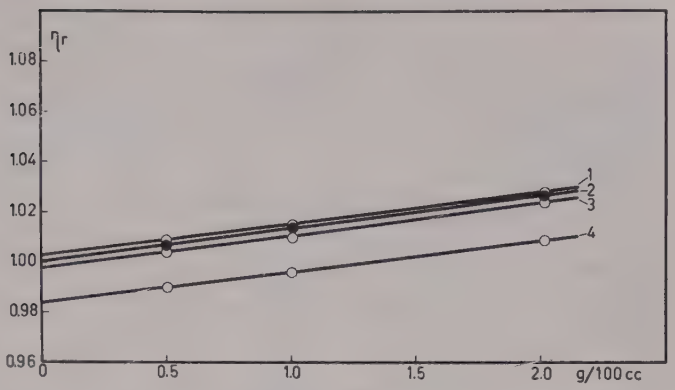

Fig. 4. Calibration of Ubbelohde viscosimeter for surface tension effects. Data for efflux bulbs no. 1, 2, 3 and 4 respectively.

The viscosities of the polymer solutions were all measured in the concentration range 0–0.3 per cent at the high end of which the surface tension showed a decrease from 71 to 56 dyne/cm. From this it was calculated that the maximum corrections would be 0.2, 0.03, 0.1 and 0.6 per cent for measuring bulbs 1–4 respectively. For bulbs 1–3 the correction lies within the experimental error and was therefore neglected, but for bulb 4 it was applied wherever necessary.

Viscosity measurements were made on a given solution by moving the viscometer between four thermostats controlled to ± 0.01°C at temperatures of 0, 15, 25, and 40°C, the flow times being recorded to 0.1 sec. for each of the four bulbs. Dilutions were made by volume in the viscometer. All solutions were filtered directly into a special pipette having negligible drainage losses and thence transferred to the viscometer. The concentrations used were so chosen as to yield relative viscosities η_r in the range from 1.1 to 1.7.

For each concentration the relative viscosity of the solution in each of the four bulbs (corrected if necessary for kinetic energy and surface tension) was plotted against the rate of shear calculated from equation (3). The best straight line was drawn through the points and extrapolated to zero gradient. Some typical examples are illustrated in Fig. 5. In almost all cases the relative viscosity obtained from measurements in bulb 4 (i.e. at the lowest velocity gradients) lay below the line through the values from the other three bulbs. This is probably caused by a systematic error and accordingly this point was neglected in the extrapolation to zero gradient. In all cases the gradient dependence was very small and as expected the dependence decreased with temperature.

After correction to zero rate of shear the η_r values were used for calculating η_{sp}/c and $(\ln \eta_r)/c$ both of which were then plotted against concentration as illustrated by the examples shown in Fig. 6. The intrinsic viscosity was taken as the common ordinate intercept for the straight lines drawn through the two sets of points; their slopes being related to one another in accordance with the mutually related equations

$$\eta_{sp}/c = [\eta] + k[\eta]^2 c \tag{7}$$

$$(\ln \eta_r)/c = [\eta] - (0.50 - k)\,[\eta]^2 c \tag{8}$$

where k is a constant characteristic of a given solvent–polymer pair and independent of the polymer molecular weight. Values found for k are given in Table 3. In all

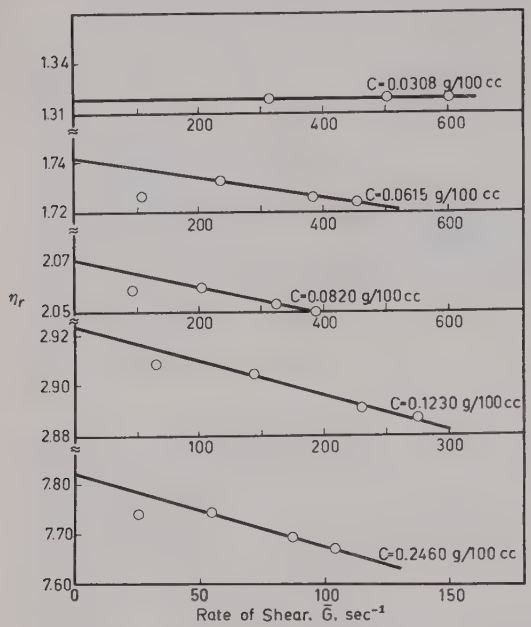

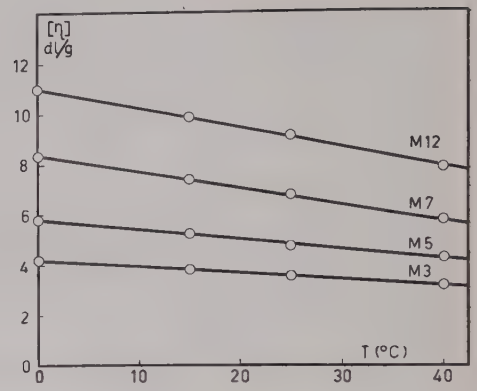

Fig. 7. Intrinsic viscosity–temperature relationships for four fractions of ethyl hydroxyethyl cellulose in water.

Fig. 5. Relative viscosity as a function of velocity gradient for ethyl hydroxyethyl cellulose (fraction M12) in water at 20°C. In the extrapolation to zero gradient the points at the lowest gradient are neglected (see text).

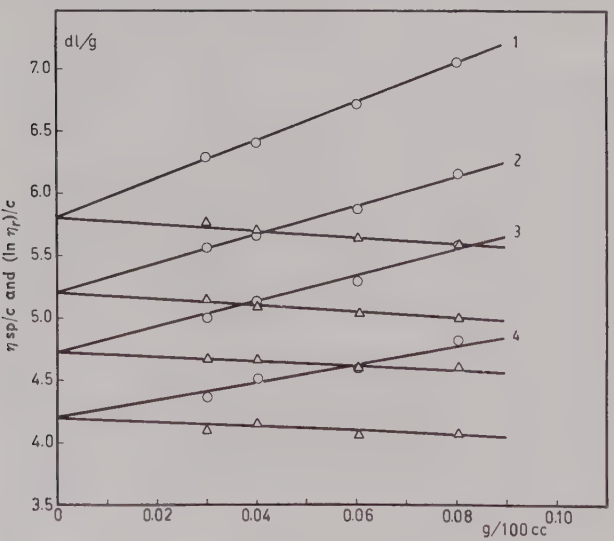

Fig. 6. The dependence of η_{sp}/c (circles) and $(\ln \eta_r)/c$ (triangles) on concentration for a fraction (M5) of ethyl hydroxyethyl cellulose in water at temperatures of (1) 0°C, (2) 15°C, (3) 25°C and (4) 40°C.

cases these plots were linear. The intrinsic viscosities are summarized in Table 3 and the complete experimental data are presented in Table 4. Plots of $[\eta]$ vs. T are shown in Fig. 7. The significance of the results will be considered later after the presentation of the molecular weight determinations.

Table 3. Intrinsic viscosity–temperature relations.

Fraction No.	Temp. °C	Incr. in $[\eta]$ on extrapolating to zero gradient %	k	$[\eta]$ dl/g	Temperature coeff. $\Delta[\eta]/\Delta T$ (dl/g deg.)
M12	0	5.8	0.50	11.00	
	15	5.4	0.43	9.86	0.080
	25	5.2	0.39	9.10	
	40	0	0.46	7.80	
M7	0	1.2	0.67	8.35	
	15	0	0.64	7.38	0.066
	25	0	0.66	6.75	
	40	0	0.75	5.70	
M5	0	0	0.44	5.80	
	15	0	0.41	5.20	0.040
	25	0	0.45	4.70	
	40	0	0.39	4.20	
M3	0	0	0.54	4.20	
	15	0	0.55	3.78	0.027
	25	0	0.51	3.49	
	40	0	0.50	3.10	

Table 4. Viscosity measurements for ethyl hydroxyethyl cellulose in water at different temperatures.

Fraction No.	c g/dl	η_{sp}/c (dl/g)			
		0°C	15°C	25°C	40°C
M3	0.1045	5.19	4.54	4.13	3.60
	0.0690	4.87	4.35	3.90	3.42
	0.0517	4.71	4.19	3.77	3.30
	0.0345	4.52	4.14	3.68	3.27
M5	0.1210	7.84	6.70	6.00	5.17
	0.0807	7.04	6.15	5.58	4.82
	0.0605	6.71	5.87	5.29	4.59
	0.0403	6.40	5.66	5.14	4.52
	0.0302	6.29	5.56	5.00	4.37
M7	0.1019	13.15	10.94	9.77	8.23
	0.0679	11.45	9.73	8.78	7.36
	0.0509	10.65	9.19	8.21	6.95
	0.0407	10.20	8.80	7.98	6.88
	0.0339	9.94	8.55	7.76	6.73
M12	0.0823	16.40	13.81	12.34	10.32
	0.0549	14.32	12.15	10.80	9.34
	0.0412	13.39	11.54	10.52	8.87
	0.0274	12.57	11.01	9.98	8.45
	0.9296	12.29	10.69	9.81	8.70
	0.0103	11.95	10.30	9.43	8.75

(4) Osmotic pressure

Osmotic pressure measurements on solutions of macromolecules are of interest primarily because they can be used for the determination of number average molecular weights, $\bar{M}_n$.

According to the classical van't Hoff law, the osmotic pressure of a dilute ideal solution is given by

$$\pi = RTc/M \tag{9}$$

where π is the osmotic pressure, c the concentration of the solution, and M the molecular weight of the solute. In the case of polymer solutions, due to intermolecular interaction, there are large deviations from ideality even at low concentrations. The reduced osmotic pressure π/c increases with concentration and extropolation to infinite dilution is necessary. This extrapolation is often complicated by the fact that the $\pi/c = f(c)$ relation is curved. On the other hand the relation is likely to be linear at very low concentrations.

The Flory Huggins theory of polymer solutions (24, 25) has provided the basis for the interpretation of the nonideal behavior of polymer solutions. According to this theory the reduced osmotic pressure may be expressed in the form

$$\frac{\pi}{c} = \frac{RT}{\bar{M}_n} + RT\,d_1(0.5-\mu)\,c/M_1 d_2^2 + \cdots \tag{10}$$

where d_1 and d_2 are the densities of solvent and solute, M_1 is the molecular weight of the solvent and μ is a solvent–solute interaction constant. This equation may also be regarded as a power series expansion of π/c which can be written in the form

$$\pi/c = RT\ [A + Bc + \cdots] \tag{11}$$

where A and B, by analogy with the theory of real gases, are known as the first and second virial coefficients respectively. In practice, terms beyond Bc are neglected.

The second virial coefficient B is related to the solvent–solute interaction and according to Flory and Krigbaum (26) is dependent on the molecular weight of the polymer and upon molecular weight heterogeneity.

Although several theoretical equations have been proposed to account for the variation of the reduced osmotic pressure with concentration, there is at present no completely satisfactory answer to the question. A review of recent developments has been given by Wall and Hiller (27).

Experimental technique and results

In choosing an instrument for carrying out the osmotic pressure measurements two problems had to be borne in mind; namely, the high surface tensions of the solutions which would necessitate large uncertain corrections to the observed osmotic pressures, and the probability of a non-linear variation of the reduced osmotic pressure with concentration, leading to difficulties in extrapolation. Both problems were avoided by the use of the interference osmometer developed by Claesson and Jacobsson (28, 29, 30). This instrument allows measurements to be made at very low concentrations and surface tension effects are eliminated by the use of wide

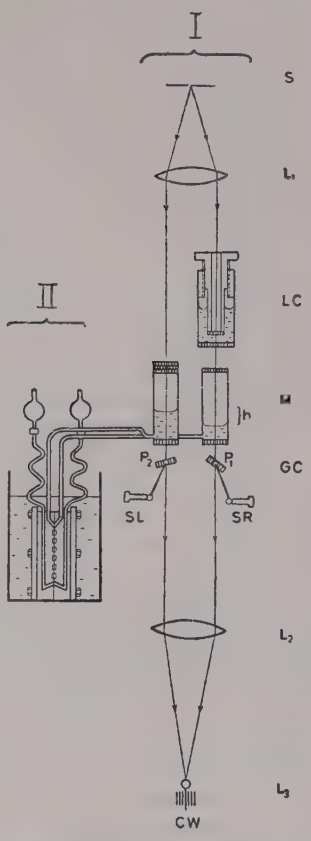

Fig. 8. Drawing showing the principal features of the interference osmometer (after Claesson, 29).

(20 mm) manometric tubes. A drawing of the apparatus is shown in Fig. 8. The osmotic cell is of the conventional Fuoss Mead type (31) in which the usual capillaries are replaced by the wide manometric tubes. A pair of light beams originating from a white light source, S, pass through the manometric tubes and produce a set of interference fringes in an ocular L 3. Changes in the difference between the liquid levels (h) in the manometer tubes cause a movement of the interference fringes in the ocular. This movement is followed by adjusting the glass compensators SL and SR and the liquid compensator LC, all of which are calibrated in terms of millimeters. The instrument is capable of an accuracy of about 10^{-3} mm of water pressure. The osmotic cell is mounted in a thermostat in which the temperature fluctuations are less than $\pm 0.005°$. The membrane used was an Ultrafeinfilter from Membranfilter Gesellschaft, Göttingen, labelled 15. Before use it was conditioned in water for a period of about one week. Measurements were carried out by a dynamic method previously used by Gee (32), Montanna and Jilk (33) and Jullander (38). The rate of solvent flow through the membrane is given by the relation

$$dh/dt = K(h - \pi). \tag{12}$$

Thus if dh/dt is determined at different positions h, and the data plotted, a straight line is obtained from which the osmotic pressure π, that is, the value of h at $dh/dt = 0$, can be found.

The reference position (i.e., the cell constant K) was first determined with water in both halves of the cell. Measurements were then made on the solutions in increasing order of concentration. The techniques of filling the cell and exchanging solutions were the same as described by Jacobsson (30). The latter author had found that the membrane could be adequately conditioned by allowing about 100 c.c. of solution to flow slowly through the cell over a period of about one hour. With the present polymer system a much longer time was required. The sequence of operations used in the present study was as follows. The solution half cell was first flushed with about 100 c.c. of the solution to be measured, and after leaving this solution in contact with the membrane for about eighteen hours, a further 150–200 c.c. was allowed to flow slowly through the cell. Before starting a measurement the solvent half cell was also flushed with a large volume of solvent. After the measurement the solution chamber was washed free of solute. The solutions used were prepared by volume dilution from a stock solution. Rate determinations were made on both sides of the equilibrium position. All measurements were made at 25°C.

A typical rate diagram is shown in Fig. 9. The interferometer was so adjusted that the extrapolated value of the reference position is zero. This adjustment was made once and for all at the beginning of the series of experiments when both half cells were filled with water. A check of the reference position after a series of measurements showed that the zero point had not changed and it was therefore not necessary to apply a correction to the observed osmotic pressures.

While the two reference lines extrapolated to the same point, they are not coincident. This effect is probably due to the difficulty of completely washing out traces of polymer in the membrane.

Ideally, all the flow lines on the rate diagram should be parallel. Within the experimental error this is true in the case of the solutions. The marked difference between the slope for the solutions on the one hand, and the solvent on the other might be explained by a diminished membrane permeability due to adsorption of polymer on the membrane.

In calculating the reduced osmotic pressures the concentrations used were those of the solutions as prepared. The effect of adsorption on the concentration was eliminated by the method of conditioning the membrane with large volumes of solution over a long period of time. Since the slopes are constant it is reasonable to assume that the adsorption was the same for each solution and that it was already complete during the initial period of conditioning. The cell contains about 7 c.c. of solution and the volume of solvent passing through the membrane in either direction during a measurement is estimated to be less than 0.03 c.c. The corresponding uncertainty in the concentration of the solution is less than 0.5 per cent and can be neglected.

One of the primary conditions for obtaining reliable osmotic pressure data is that the membrane must be strictly semipermeable. Because of the small concentrations used in the present experiments it would have been very difficult to ascertain the existence of solute permeation through the membrane by the evaporation to constant weight of solution or solvent after the measurements. Nevertheless, the good linearity of the rate diagrams indicates that there was no leakage in the measurements described here.

Lang (34) has shown that if the osmotic pressure is to be expressed in terms of solvent, but is measured as the difference between the height of a column of solvent and a column of solution, a correction has to be applied to allow for the different

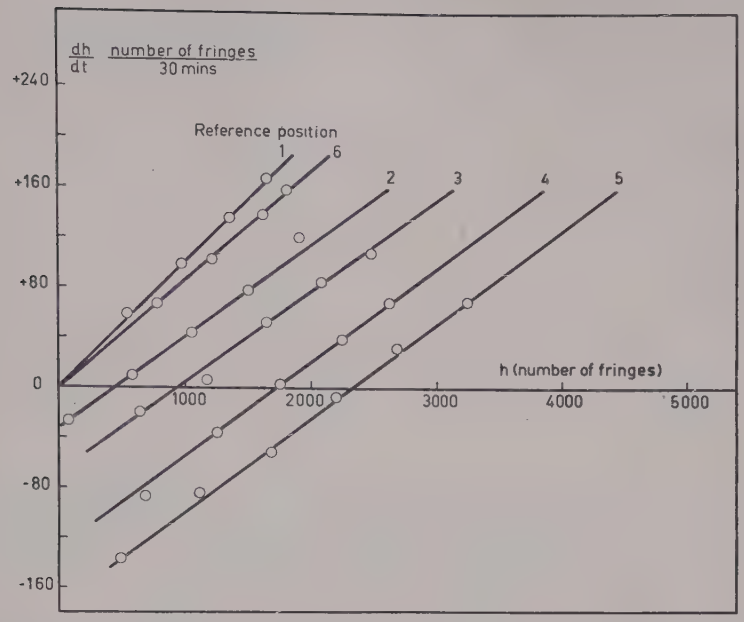

Fig. 9. Typical rate diagram showing curves for the reference position (1) before experiments, (6) after experiments, and for different concentrations of a fraction (M7) of ethyl hydroxyethyl cellulose in water. (577.6 fringes = 1 mm.)

Table 5. Osmotic pressures for aqueous solutions of ethyl hydroxyethyl cellulose at 25°C.

Fraction No.	c g/100 c.c.	π cm H_2O	$\pi/c \times 10^{-4}$ dyn. cm g^{-1}	$M_n \times 10^{-3}$	$B \times 10^4$ mol. cm^3 g^{-2}
M12	0.292	0.538	18.0		
	0.120	0.191	15.5		
	0.0700	0.107	15.1		
	0		14.0	176	5.45
M7	0.173	0.403	22.8		
	0.126	0.298	23.2		
	0.0754	0.159	20.8		
	0.0377	0.0763	19.9		
	0		19.2	128	7.63
M5	0.167	0.606	35.6		
	0.0791	0.270	33.5		
	0.0475	0.159	32.9		
	0		31.8	77.6	9.80

density of the solution. The corrected osmotic pressure is given by

$$\pi = h\, d_c + H\,(d_c - d_0) \tag{13}$$

where h is the observed equilibrium height difference, H is the height of the solution column, and d_c and d_0 are the densities of the solution and solvent respectively.

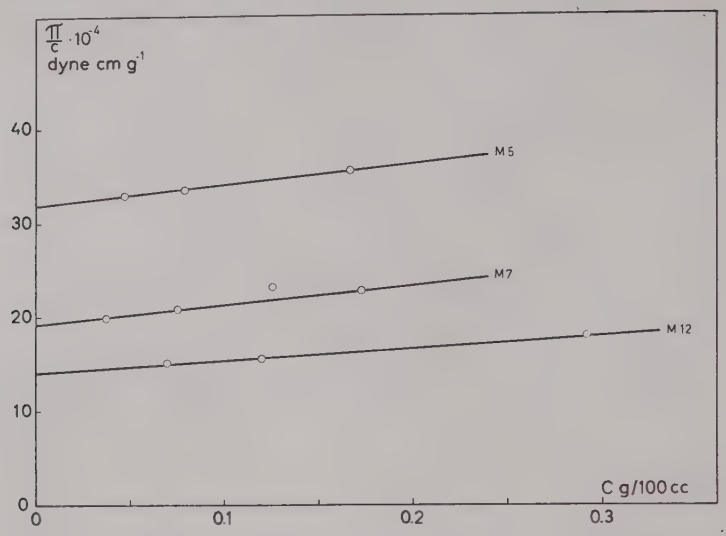

Fig. 10. Reduced osmotic pressure as a function of concentration for three fractions of ethyl hydroxyethyl cellulose in water.

In the Fuoss Mead osmometer, H is measured from the centre of the vertical membrane and in the present case is equal to 22 cms. Density measurements, to be described later, revealed that the relation between density and concentration for aqueous solution of ethyl hydroxyethyl cellulose at 25°C can be represented by the formula

$$d_c = d_0 + K c \tag{14}$$

where K is a constant and c is expressed in g/100 c.c. From equations 13 and 14, and forming the limiting value of the reduced osmotic pressure according to equation 11 we obtain

$$\frac{RT}{M} = \lim_{c \to 0} \frac{h\, d_c}{c} + HK. \tag{15}$$

The correction term is thus independent of concentration and its neglect in the case of high molecular weight materials may lead to considerable error. In the present study it has been applied in all cases.

A further correction for dispersion effects (30) amounting to a maximum of about one per cent has been applied to the data.

The results obtained are collected in Table 5 and by way of illustration the reduced osmotic pressure is plotted against concentration in Fig. 10. The density correction term in equation 15 amounted to 0.5, 0.4 and 0.2 per cent of $\lim_{c \to 0} \pi/c$ for samples 12, 7 and 5 respectively. The second osmotic virial coefficients calculated from the slopes of $\pi/c = f(c)$ plots are also given in Table 5.

(5) Specific refractive index increment

A knowledge of the specific refractive index increment, dn/dc, is necessary in the experiments to be described hereafter. Measurements were made with the aid of

Table 6. Refractive index increment of fractions of ethyl hydroxyethyl cellulose in water. Wavelength 546 mμ

Fraction No.	c g/100 c.c.	$\Delta n \times 10^4$	dn/dc c.c./g
M3	0.986	14.43	0.146
M5	1.099	16.19	
	0.746	10.86	0.146
M7	0.535	8.034	
	0.799	12.024	
	1.095	16.830	0.151
M12	0.568	8.480	
	1.098	16.255	0.148

a double prism differential refractometer having an optical system similar to that of an ordinary spectrometer. The displacement of the slit image was measured with a travelling microscope, the reading accuracy being about $\pm 3 \times 10^{-7}$. During the calibration of the instrument with aqueous solutions of sodium sulphate, the reproducibility of the values was $\pm 3 \times 10^{-6}$. The refractive index increment Δn was measured at a wave-length of 546 mμ for a series of concentrations (between 0.3 and 1.1 per cent) of each fraction. The results are given in Table 6. The differences observed between the values of dn/dc are probably due to variations in the quality of the solvent. For similar ethyl hydroxyethyl celluloses Jullander reported a value of 0.146 c.c./g for dn/dc.

(6) Sedimentation

Sedimentation studies were carried out in a Svedberg oilturbine ultracentrifuge. Details concerning the construction and operation of this instrument have been given in a monograph by Svedberg and Pedersen (35).

The course of the sedimentation was followed by the Lamm scale method (36). A scale with lines ruled perpendicular to the direction of sedimentation is photographed through the cell. The concentration gradient at the sedimenting boundary produces a shift of the scale lines from their original positions on the photographic plate. This displacement, Z, is given by

$$Z = G\, a\, b\, \alpha dc/dx \tag{16}$$

where G is a photographic enlargement factor, a is the length of solution through which the light beam passes, b is the distance from the scale to the middle of the cell and α the refractive index increment dn/dc of the solute. Thus if the refractive index increment may be regarded as constant, and this is usually the case, the concentration may be obtained by the integration of the $Z(x)$ curve. On a $Z(x)$ curve, every sedimenting boundary is represented as a peak and the sedimentation velocity is calculated by determining the position of this peak at different times from the start of the experiment. The sedimentation constant, s, is defined by the equation

$$s = (dx/dt)/\omega^2 x \tag{17}$$

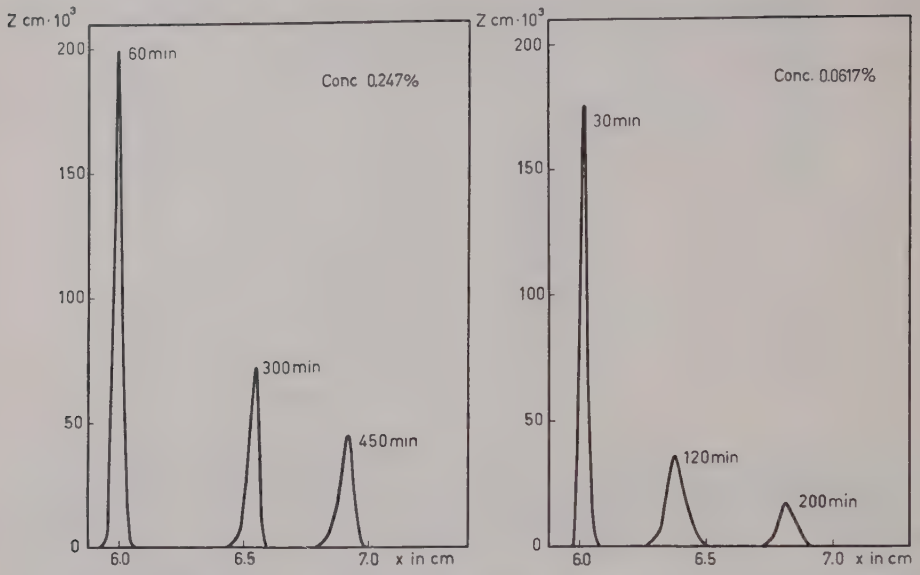

Fig. 11. Sedimentation diagrams for aqueous solutions of ethyl hydroxyethyl cellulose fraction M12. x = distance from the centre of rotation, Z = scale-line displacement. The curves to the left and right correspond to a scale distance of 10 and 40 respectively.

where x is the distance from the centre of rotation, ω is the angular velocity and t the time in seconds.

The evaluation of the sedimentation constant permits the calculation of the molecular weight by the classical Svedberg relation (35)

$$M = \frac{RTs}{D(1 - V\varrho)} \tag{18}$$

where R is the gas constant, T the absolute temperature, D the diffusion constant, V the partial specific volume of the solute and ϱ the density of the solvent.

As a polydisperse substance sediments in a centrifugal field, the width of the boundary increases progressively with the distance, x, of sedimentation. Gralén (37) proposed the quantity, dB/dx at zero concentration, as a relative measure of the polydispersity of the sample. B is defined as the average width of the curve and is obtained by dividing the area under the peak by its maximum height.

The sedimentation measurements were made at a speed of 1000 r.p.s., corresponding to a centrifugal force of 260,000 times gravity. The temperature of the rotor was regulated by cooling the turbine oil and the temperature was recored by means of a thermocouple placed immediately adjacent to the rotor. Measurements were generally made at a temperature of about 26°C. The sedimentation constants have been reduced to the standard temperature of 20°C according to the relation (35)

$$s_{20} = s_t \frac{\eta_t}{\eta_{20}} \frac{(1 - V_{20}\varrho_{20})}{(1 - V_t\varrho_t)} \tag{19}$$

where s_{20} and s_t are the sedimentation constants at 20° and $t°$ respectively, η_{20} η_t, and ϱ_{20}, ϱ_t are the viscosities and densities of the solvent at the corresponding temperatures and V is the partial specific volume of the solute.

As previously found by Jullander (8) the sedimentation curves showed well-defined and fairly symmetrical peaks. A few typical examples are shown in Fig. 11. The position of the sedimenting boundary was determined from the maximum point of the curve and the sedimentation constants were calculated from the slope of a $\ln x_t$ vs. t plot, where x_t is the position of the boundary at the time t. The values thus obtained were reduced to the standard value at 20°C, as described above.

Since the fractions used were not very sharp, the question arises as to what type of mean value s is obtained by the method of calculation used. For symmetrical sedimentation curves a weight average sedimentation constant s_w is obtained when the sedimentation velocity is calculated from the movement of the maximum point of the curve (38). It is therefore expected that the sedimentation constants reported here should lie very close to a weight average.

In a number of instances, especially at low concentrations and late exposures, there were disturbances in the sedimentation which made it impossible to obtain any significant results from the calculation of Gralén's dB/dx.

Extrapolation of the sedimentation constant to infinite dilution

The variation of the sedimentation coefficient with concentration presents a rather uncertain and complex situation. As the concentration is reduced, s increases sharply, due to decreased molecular interference. The concentration range in which spherical molecules sediment independently can usually be reached experimentally, but for thread-like molecules of the same molecular weight, s is still increasing rapidly at the lowest attainable concentrations. As there is at present no complete theory covering the dependence of s on c, the extrapolation must usually be made semi-empirically. It is then necessary to rely heavily on the s-values at the lowest concentrations and these are precisely the least accurately known ones.

Kermack *et al.* (39) and more recently Burgers (40) have given a hydrodynamic treatment of the concentration dependence of sedimentation for spherical particles in dilute solutions. They showed that the reciprocal of the sedimentation constant should increase linearly with the concentration, and this has been found to be true for a number of systems (cf. e.g. ref. (41)).

Gralén (37) has proposed the relation

$$s = s_0 \ (1 + Kc)^{-1}$$

where s_0 is the sedimentation constant at infinite dilution and K is a constant. He found that this equation, which leads to a linear plot between s and sc, applied rather well to his cellulose data. However, more recent work has shown that it is only of limited applicability (38).

The sedimentation constant may be related to the frictional coefficient f by means of the Svedberg equation (35)

$$s = (M/N)\,(1 - V\varrho)/f \qquad (20)$$

where N is Avogadro's number and ϱ is the density of the solution. The frictional coefficient may then be represented by a power series in concentration (42), thus

Table 7. Sedimentation–concentration data for ethyl hydroxyethyl cellulose in water at 20°C.

Fraction No.	Conc. in g/dl		$s_{20} \times 10^{13}$	η/η_0	k	$-k'$	$s_0 \times 10^{13}$
	c_0	$(c)_{av}$					
M12	0.2470	0.214	1.36	7.82			
	0.1650	0.144	1.56	4.12			
	0.1235	0.113	1.69	2.91			
	0.0823	0.088	1.92	2.07			
	0.0617	0.048	2.10	1.74			
	0.0463	0.036	2.34	1.50			
	0.0308	0.023	2.60	1.31			
					2.96	4.83	3.00
M7	0.3058	0.308	1.25	7.10			
	0.2039	0.171	1.39	3.90			
	0.1529	0.125	1.52	2.80			
	0.1019	0.093	1.76	2.02			
	0.0764	0.059	1.85	1.70			
	0.0306	0.021	2.38	—			
					2.70	4.94	2.63
M5	0.2416	0.226	1.29				
	0.2013	0.174	1.32				
	0.1611	0.129	1.38				
	0.1208	0.108	1.49				
	0.0805	0.061	1.65				
	0.0403	—	1.73				
					2.50	4.67	2.32
M3	0.3106	0.274	1.11				
	0.2071	0.199	1.19				
	0.1553	0.140	1.14				
	0.1035	0.084	1.31				
	0.0776	0.073	1.43				
	0.0444	—	1.60				
					3.11	5.86	2.00

$$f = f_0 (1 + kc + k'c^2 + \cdots) \tag{21}$$

where k and k' are constants characterizing the concentration dependence of the frictional coefficient. From equations (20) and (21) the sedimentation constant is therefore given by

$$s = s_0(1 + kc + k'c^2)^{-1}. \tag{22}$$

Newman *et al.* (43) found that such an equation gave a very accurate representation of their data for cellulose nitrate in acetone over a fairly wide concentration range. They determined the constants graphically by a difference method from the relation

$$(1/s_2 - 1/s_1)/(c_2 - c_1) = k + k'(c_1 + c_2) \tag{23}$$

where the subscripts 1 and 2 refer to any pair of data. Following this, s_0 was evaluated graphically from plots of $(1/s - k'c^2)$ vs. c.

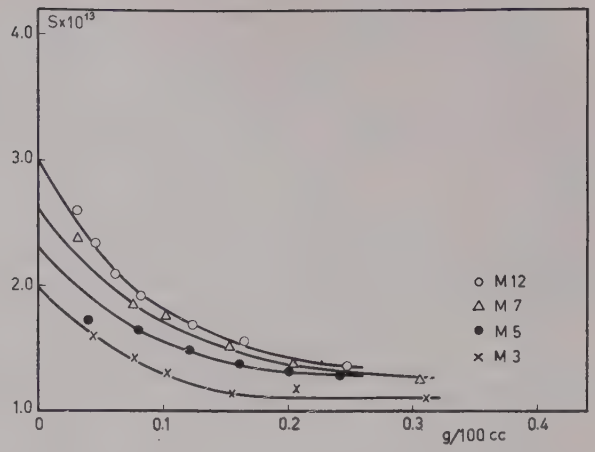

Fig. 12. Variation of sedimentation constant with concentration for fractions of ethyl hydroxyethyl cellulose in water.

Lauffer (44) has shown that the variation of the sedimentation constant with concentration can be corrected for the viscosity of the solution by the factor $s\eta/\eta_0$. This latter expression should be independent of the concentration of the solution. A similar conclusion was reached by Powell and Eyring (45). This seems to work fairly well with proteins and certain synthetic polymers but in most cases leads to an overcorrection, the corrected sedimentation constant increasing with concentration. The method is nevertheless interesting from another point of view. Since $\lim_{c=0} s$ must be identical with $\lim_{c=0} s\eta/\eta_0$, the plotting of both $s\eta/\eta_0 = f(c)$ and $s = f(c)$ on the same diagram may serve to reduce the uncertainties in the extrapolation procedure (38).

It has been pointed out by a number of authors that in determining the relationship between s and c, the value of c to be used is the average value of the concentration at the sedimenting boundary and not the concentration of the solution prepared for the run. Because of the sector-shape of the ultracentrifuge cell and the change of centrifugal force with distance from centre of rotation, the concentration at any cross-section of the sedimenting column diminishes during the run in accordance with the formula (ref. 35)

$$c_t = c_0 (x_0/x_t)^2$$

where t denotes the time from the beginning of the sedimentation. Concentrations, as determined by measuring the areas under the peaks and correcting for dilution effects as indicated above, were generally 10–25 per cent less than the original concentrations. There were considerable difficulties in knowing where to place the base lines of the curves and since furthermore the peaks were very sharp and narrow, the differences noted are certainly within the uncertainty in the area under the peaks. For this reason the original concentrations were corrected for the dilution effect and used in determining the relationship between s and c. Both concentrations are given in Table 7 where also the sedimentation constants of the various fractions are summarized. For fractions M12 and M7 the relative viscosities, measured as previously described, at each concentration are also given in the table.

Fig. 12 shows a plot of s against c for each fraction. It is apparent that the con-

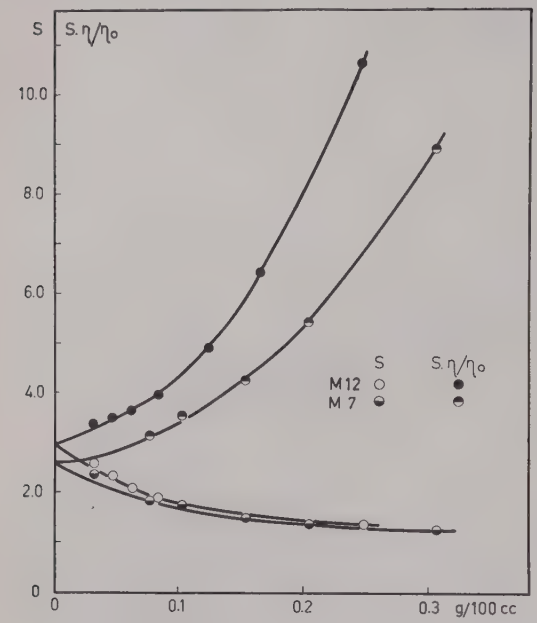

Fig. 13. Sedimentation constant s, and $s\,\eta/\eta_0$ as a function of concentration, c, for two fractions of ethyl hydroxyethyl cellulose in water. s in Svedberg units.

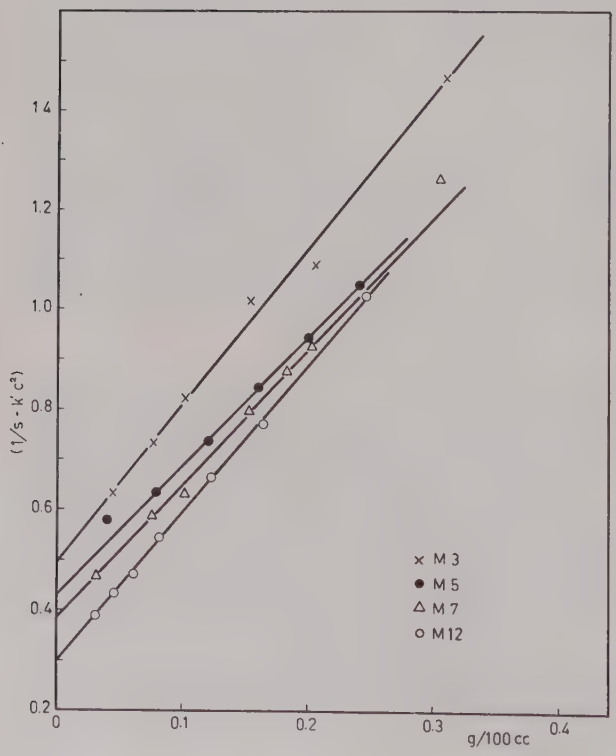

Fig. 14. Linear extrapolation of sedimentation constants to infinite dilution for fractions of ethyl hydroxyethyl cellulose in water.

centration dependence of s is rather marked. For the three highest fractions already at a concentration of 0.2 per cent the sedimentation constants are almost identical and it is clear that above this concentration no free sedimentation can occur.

Such effects have previously been observed (38, 41, 46) and may be explained by assuming that the more slowly sedimenting molecules hinder the motion of the larger ones and completely dominate the observed sedimentation rate at higher concentrations (46).

It is also evident that the sedimentation velocity does not differ markedly from one fraction to another. The molecular weight of fraction M12 is about three times greater than that of M3, yet the sedimentation velocities differ by only fifty per cent. This slight dependence of the velocity on the molecular weight has also been observed for another water soluble cellulose ether, namely methyl cellulose (5).

One could not be sure that the curves would not bend up sharply at the lower concentrations where it was impractical to carry out measurements. However, by plotting $s\eta/\eta_0 = f(c)$ and $s = f(c)$ on the same diagram some of the uncertainty in the extrapolation procedure was removed. An example is given in Fig. 13.

While plots of $1/s$ against c were non-linear, the quadratic equation was found to represent the data rather well and yielded values of s_0 in close agreement with those of the former procedure. Fig. 14 shows the results obtained by this method of extrapolation. The constants k and k' were determined as mentioned above.

(7) Diffusion

The diffusion experiments were carried out with the aid of the Lamm scale method (cf. page 537). When the scale line displacement Z is plotted against the scale line position x, a frequency curve is obtained which in the case of a monodisperse substance diffusing from an initially sharp boundary between solution and solvent conforms to Wiener's equation (47)

$$\frac{dn}{dx} = \frac{n_1 - n_0}{2\sqrt{\pi D t}} e^{-x^2/4Dt}. \tag{24}$$

Here D is the diffusion constant, x the distance from the original boundary, t the time after the beginning of the diffusion, and $n_1 - n_0$ is the difference in refractive index between solution and solvent. The scale method of Lamm gives dn/dx as a function of x. From equation (24) a number of formulae have been derived for the calculation of D (36).

In the case of a polydisperse substance the calculation of the different mean values of the diffusion coefficient from the experimentally obtained diffusion curve is based upon the following formulae given by Lamm (36) and Gralén (37)

$$D_A = A^2/4\pi t H \tag{25}$$

$$D_m = m_2/2At \tag{26}$$

where A is the area between the diffusion curve $dn/dx = f(x)$, and the x axis, H is the maximum height of the curve, and m_2 is the second moment around the vertical axis through the arithmetic mean of the curve. D_A and D_m are denoted as the diffusion coefficient according to the "area" and moment method respectively.

The physical significance of these two diffusion constants has been discussed in detail by Gralén (37). For a polydisperse substance D_A represents a mean value which lies between a number and a weight average, while D_m is a weight average of the different constants of the constituents. Theoretically, for a polydisperse substance $D_m > D_A$ and the ratio D_m/D_A, equal to unity for a monodisperse substance, has been proposed by Gralén (37) as a measure of polydispersity. However, as he has also pointed out, a very high accuracy is necessary for this calculation. Due caution must therefore be exercised in applying this method.

It is often advantageous to transform the arbitrary coordinates of the experimentally observed diffusion curve into normal coordinates (normal) curve as a means of comparing the experimental curves referring to the different times of diffusion in the same dimensionless units, or of comparing an experimental curve with the corresponding ideal Gaussian curve. This is ordinarily accomplished by the transformations

$$\xi = x/2\sigma \quad \text{and} \quad \psi = \frac{5\sigma}{\Phi}\left(\frac{dn}{dx}\right)\alpha \tag{27}$$

where α is a constant of the optical system, Φ is the area of the (dn/dx) versus x curve, $\sigma = \sqrt{2Dt}$ and 2 and 5 are arbitrary constants chosen for convenience in plotting. The ideal curve, which may be plotted from mathematical tables, has the form

$$\psi = \frac{5}{\sqrt{2\pi}} e^{-2\xi^2}. \tag{28}$$

The methods of carrying out this calculation have been discussed by Beckmann and Rosenberg (48).

Deviations from ideal behaviour in the experimental curves may be due to polydispersity in the sample or to a dependence of the diffusion rate on concentration. Lamm (36) has shown that polydispersity causes the ordinates of the normal curve in the vicinity of $x = 0$ to be higher than those of the ideal Gaussian curve. A concentration dependence of the diffusion rate reveals itself as a lateral deviation of the experimental normalized curve from the ideal. Qualitatively, a positive concentration dependence is manifested by a displacement or skewness of the experimental curve toward the solvent side of the original boundary position, while curves with a negative concentration dependence are displaced toward the solution side.

Experimental methods and results

The diffusion measurements were carried out in two different cells which made possible the formation of a very sharp and plain boundary between solution and solvent. One of these cells was of the flat Claesson type (49), while the other was of a type developed by Claesson *et al.* during an extensive investigation of methods of high precision diffusion. This cell differs from the original design in that the upper half of the diffusion chamber forms part of a round block which can be moved into coincidence with the lower half of the chamber by means of a worm gear. Fig. 15 shows a photograph of the cell. Full details will be given elsewhere. As a check on the overall validity of the experimental technique measurements were carried out

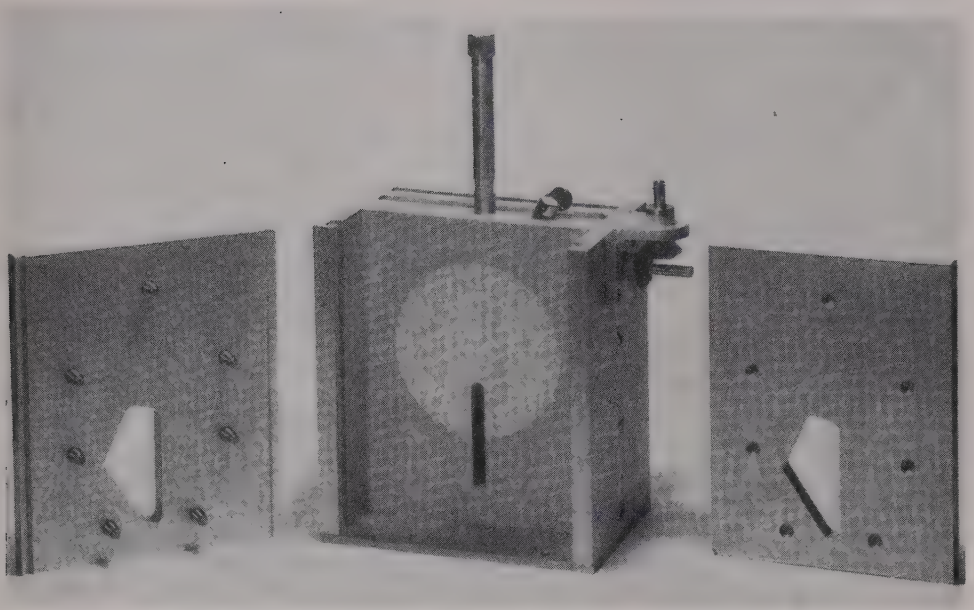

Fig. 15. Photograph of the diffusion cell with circular sliding surfaces.

with sucrose solutions. Gosting and Morris (50) have reported a value of $D_{24.90} = 51.48 \times 10^{-7}$ cm^2/sec. determined by the Gouy interference technique. When corrected to 20° this value becomes 45.07×10^{-7} cm^2/sec. With both cells this value was reproduced within 3 per cent. Best results were obtained when the sliding surfaces were lubricated with high quality silicone grease.

The measurements were carried out at a temperature of 22.0 ± 0.01°C for at least four concentrations of each fraction. Since the diffusion constant depends upon the viscosity of the medium the observed values were reduced to the standard temperature of 20°C by means of the formula

$$D_{20} = D_t \frac{\eta_t}{\eta_{20}} \frac{293}{T} \tag{29}$$

where D_{20} is the diffusion coefficient in water at 20°C, D_t the observed diffusion coefficient and η_t/η_{20} the ratio of the viscosity of the solution investigated to that other of pure water at 20°C.

Great care was taken to have thermal equilibrium between the liquids in the two chambers of the cell before forming the boundary. Exposures were taken at intervals of about three hours over a period of 50–75 hours depending on the concentration of the solution. The measurements on fraction M7 were carried out in the flat cell and all other measurements were performed in the round cell.

The values of D_A and D_m were calculated from the slopes of plots of A^2/H^2 and m_2/A respectively as a function of time. These plots were linear and intercepted the t-axis at or close to the origin, thereby suggesting that the experiments had proceeded undisturbed and without delay and also that sharp boundaries had been formed between solution and solvent.

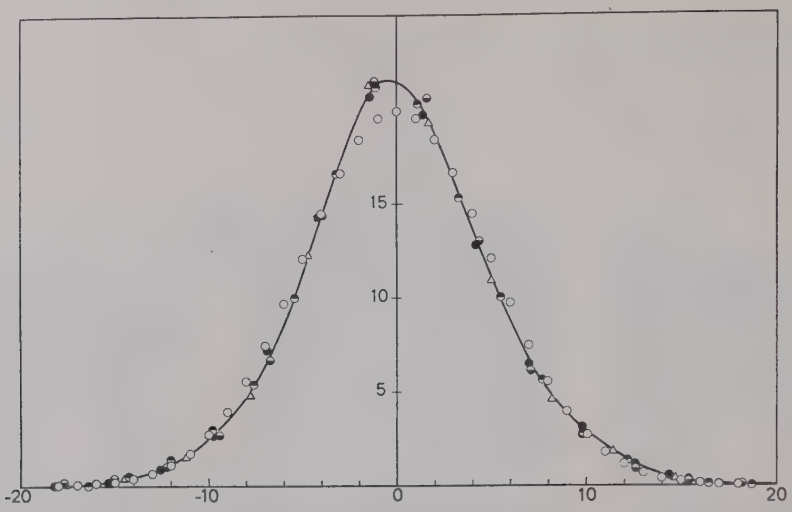

Fig. 16. The diffusion curve in normal coordinates of ethyl hydroxyethyl cellulose fraction M3 in water. The curve connects the experimental points obtained from different exposures. The open circles indicate the corresponding normal curve.

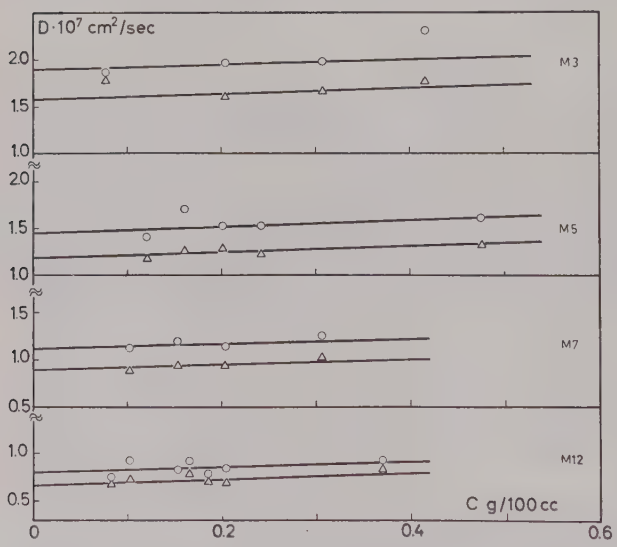

Fig. 17. Concentration dependence of D_A (triangles) and D_m (circles) for four fractions of ethyl hydroxyethyl cellulose in water.

Table 8 gives the results of the determinations. The values are given in units of cm^2/sec. In Fig. 16 the normal diffusion curve for one of the fractions is compared with the corresponding ideal Gaussian curve. The slight skewness of the experimental curve towards the solvent side indicates a small positive concentration dependence. In agreement with theory the values of D_m are in all cases higher than D_A and the rather high D_m/D_A values (see Table 8) may be taken as an indication that the fractions are quite polydisperse.

Table 8. Diffusion constants for different fractions of ethyl hydroxyethyl cellulose in water at 20°C. Concentration in g/100 c.c.

Fraction No.	Conc.	$D_m \times 10^7$	$D_A \times 10^7$	D_m/D_A	$k_D \times 10^7$
M3	0.417	2.30	1.76	1.31	
	0.308	1.98	1.66	1.19	
	0.205	1.97	1.60	1.23	
	0.078	1.87	1.78	1.05	
	0	1.9	1.6	1.20	0.3
M5	0.475	1.60	1.32	1.25	
	0.242	1.52	1.22	1.24	
	0.201	1.53	1.29	1.19	
	0.161	1.70	1.26	1.35	
	0.121	1.40	1.17	1.20	
	0	1.4	1.2	1.2	0.3
M7	0.102	1.12	0.88	1.27	
	0.153	1.19	0.93	1.28	
	0.204	1.13	0.94	1.20	
	0.306	1.24	1.02	1.21	
	0	1.1	0.90	1.2	0.3
M12	0.370	0.92	0.83	1.11	
	0.204	0.83	0.68	1.22	
	0.185	0.77	0.69	1.12	
	0.165	0.91	0.77	1.18	
	0.153	0.82	0.79	1.04	
	0.102	0.92	0.72	1.28	
	0.082	0.74	0.66	1.12	
	0	0.8	0.6	1.3	0.3

It is often found that the concentration dependence of the diffusion constant may be represented by the linear equation

$$D = D_0(1 + K_D\, c) \tag{30}$$

where D and D_0 are respectively the diffusion constant at any concentration c and at infinite dilution and K_D is an empirical constant. By assuming such a linear dependence Gralén (37) has shown that the value of D_m may be corrected to zero concentration by the equations

$$D_m = D_0\left(1 + \frac{K'_D\, c}{2}\right) \tag{31}$$

$$D_0 = D_m + \frac{A\, M_0}{4\, H\, T} \tag{32}$$

where K'_D is a constant independent of molecular weight and M_0 is the displacement of the maximum ordinate at time t. The use of these equations is considered to be theoretically unsound in the present case due to the previously mentioned necessity of including a quadratic concentration term in the concentration dependence of the frictional coefficient.

In all cases the diffusion constant was a linear function of concentration thus permitting graphical extrapolation to infinite dilution. In Fig. 17 both D_A and D_m are plotted against concentration.

Within the experimental error all the curves have the same slope. The value of K_D in equation 30 is given in Table 8.

(8) Partial specific volume

In order to calculate molecular weights from sedimentation and diffusion data, it is necessary to know the partial specific volume of the substance in solution. This was determined from density measurements on solutions of each of the fractions studied. The measurements were made at $20 \pm 0.01°C$ and in the concentration range 0.3–2 per cent. The pycnometer used was a cylindrical glass vessel holding about 30 c.c. The neck was made of capillary tubing of about 1 mm diameter and a well-fitting ground-glass cap was placed over the exit. During the filling, which was accomplished by means of a syringe, air bubbles were easily formed and had to be carefully removed before weighing. Buoyance corrections were applied throughout.

The solutions used were prepared by dilution from a stock solution from which traces of salt had been removed by electrodialysis. The concentration of each solution was determined by the method previously described (see page 526).

The partial specific volume was calculated from the formula

$$V = v\left(1 - \frac{1-p}{m}\frac{dm}{dp}\right) \tag{33}$$

(cf. Kraemer in ref. (35)) where v is the specific volume of the solution, m is the weight of the pycnometer content, and p the concentration of the solution expressed as a weight fraction. dm/dp was determined by the method of least squares from the slope of an m vs. p plot. In all cases this function was linear. The complete results with weighted averages are given in Table 9.

(9) Molecular size and shape from sedimentation-diffusion

Molecular weights, $\bar{M}_{ww}$ (weight–weight average) were calculated from the sedimentation–diffusion measurements according to equation (18) using the extrapolated values of s and D_m given in Tables 7 and 8, and the partial specific volumes of Table 9. The results are given in Table 10. As previously pointed out the values of s_0 and D_0 are close to weight averages and it should be noted that the molecular weight thus obtained is, according to Jullander (38), somewhat less than a true weight average. It is common experience that the most serious limiting factor in the determination of molecular weight by this method is the uncertainty in the value of D_0. In the case of sample M12 this is especially true since the diffusion constants are so low that a small error in the extrapolation may lead to a considerable error in the molecular weight. Nevertheless, as will be seen later, the values obtained here are in substancial agreement with the closely related weight average given by another method and are therefore probably correct within about 10 per cent.

From the sedimentation and diffusion measurements it is possible to derive some information about the shape and dimensions of the molecules in solution (35).

Table 9. Partial specific volume of ethyl hydroxyethyl cellulose in water at 20°C.

Fraction No.	$p \times 10^2$	m	v	V
M12	0	29.0603	1.0018	0.7053
	0.5674	29.1085	0.9983	0.7050
	1.0950	29.1545	0.9968	0.7059
Mean				0.705
M7	0	29.0603	1.0018	0.7034
	0.3055	29.0864	0.9991	0.7027
	0.5342	29.1069	0.9984	0.7031
	0.7974	29.1310	0.9976	0.7035
	1.0915	29.1531	0.9968	0.7041
	1.4561	29.1863	0.9957	0.7047
Mean				0.703
M5	0	29.0603	1.0018	0.7105
	0.4907	29.1011	0.9986	0.7101
	0.7445	29.1216	0.9979	0.7105
	1.0906	29.1525	0.9968	0.7110
	1.4590	29.1835	0.9958	0.7117
Mean				0.711
M3	0	29.0603	1.0018	0.7210
	0.3106	29.0845	0.9992	0.7202
	0.6536	29.1132	0.9982	0.7207
	0.9838	29.1384	0.9973	0.7213
	1.4253	29.1756	0.9960	0.7219
	1.9186	29.2165	0.9946	0.7226
Mean				0.721

Table 10. Molecular constants of ethyl hydroxyethyl cellulose as derived from sedimentation–diffusion.

Fraction No.	$M \times 10^{-3}$	f/f_0	l/d	$\frac{l}{\bar{A}}$	$\frac{d}{\bar{A}}$	l_{max}	l/l_{max}
M12	310	6.0	220	3300	15	7600	0.43
M7	200	5.1	160	2200	14	4900	0.45
M5	140	4.1	100	1500	15	3400	0.44
M3	92	3.8	86	1100	13	2200	0.50

For spherical unhydrated particles of molecular weight M, the molar frictional coefficient f_0 calculated from Stokes's law is given by

$$f_0 = 6\pi\eta N \left(\frac{3MV}{4\pi N}\right)^{\frac{1}{3}} \tag{34}$$

where η is the viscosity of the solvent and the other symbols are as previously

defined. On the other hand the frictional coefficient may also be calculated from the sedimentation and diffusion constant according to the expression

$$f = \frac{RT}{D} = \frac{M(1 - V\varrho)}{s}. \tag{35}$$

If the experimental values are reduced to the basis of water at 20°C, equations 34 and 35 may be combined to yield

$$f/f_0 = 10^{-8}\left(\frac{1 - V\varrho}{D_{20}^2 s_{20} V}\right)^{\frac{1}{3}}. \tag{36}$$

When the frictional ratio f/f_0 is equal to unity it indicates that the molecules are spherical and unhydrated. On the other hand if $f > f_0$ it implies molecular hydration, asymmetrical molecules or a combination of both factors.

Herzog, Illig and Kudar (51) have shown that, assuming the molecule to be unhydrated and to have the shape of a prolate spheroid of length l and thickness d, the frictional ratio is related to the axial ratio l/d by means of the equation

$$f/f_0 = \frac{\sqrt{1 - p^2}}{p^{\frac{2}{3}} \log\left(\frac{1 + \sqrt{1 - p^2}}{p}\right)}. \tag{37}$$

Svedberg and Pedersen (35) and Gralén (37) have given tables for f/f_0 as a function of l/d.

The length and diameter of the assumed ellipsoid are related to the molecular weight and partial specific volume by the formula

$$\frac{\pi l d^2}{6} = \frac{MV}{N}. \tag{38}$$

From this and the value of l/d, the absolute values of l and d may be evaluated. Taking the length of the polymerizing unit, that is the glucose residue, to be 5.15 Å, the length of a fully stretched molecule can be calculated from the degree of polymerization Z according to the relation

$$l_{max} = 5.15\, Z.$$

Values of f/f_0, l/d, l and d calculated from these relationships are given in Table 10. In the absence of a knowledge of the state of hydration of the molecules in solution the only definite conclusion which may be drawn is that the molecules are non-spherical. However, as it is unrealistic to believe that the strong deviations from spherical shape are due in any marked degree to molecular hydration, we may tentatively assume that the molecules are strongly asymmetrical. A comparison of l and l_{max} indicates that in solution the molecules are coiled to about $\frac{1}{2}$ of their fully extended length. It must be emphasised that the application of this model is highly questionable in the present case and the dimensions given must therefore be taken with considerable reservation. Other methods which give a more accurate and unambiguous description of the state of the molecule in solution will be considered later.

(10) Sedimentation equilibrium

When a solution of a high-molecular substance is subjected to a low centrifugal field a state of equilibrium may finally be established in which, for every level in the cell, the rate at which the molecules are sedimented outwards is balanced by the rate at which they diffuse inwards. From a knowledge of the concentration distribution in the cell at equilibrium the molecular weight may be computed according to the formula

$$M = \frac{2RT \log (c_2/c_1)}{(1 - V\varrho)\omega^2(x_2^2 - x_1^2)} = \frac{RT(dc_x/dx)}{(1 - V\varrho)\omega^2 x c_x} \tag{39}$$

where c_1, c_2 and c_x are respectively the concentrations at the distances x_1, x_2 and x from the centre of rotation and the other symbols have the previously stated significance.

When, as in the present case, the Lamm scale method is used to determine the variation of concentration with distance in the cell, it is necessary to convert the scale line displacement (Z) versus distance (x) curve to a concentration versus distance curve in order to apply equation (39) directly. However, the molecular weight may also be calculated from the alternate formula

$$M = \frac{2RT \ln Z_2 x_1 / Z_1 x_2}{(1 - V\varrho)\omega^2(x_2^2 - x_1^2)} \tag{40}$$

where Z_1 and Z_2 are the scale line displacements at the points x_1 and x_2 respectively.

The above equations give the true molecular weight only for substances which are monodisperse and whose solutions exhibit ideal thermodynamic behavior.

When the system is polydisperse each molecular species sets up its own equilibrium independently of the others and thus the values of M obtained vary with the position x in the cell. Under these circumstances a weight average value of the molecular weight, $\bar{M}_w$, for the whole sample may be obtained from the expression

$$\bar{M}_w = \frac{\int M_{wx} c_x x \, dx}{\int c_x x \, dx} \tag{41}$$

where M_{wx} is calculated from equation 39 in its differential form and where the summation is extended over the entire length of the solution in the cell.

It is also possible to construct the so-called Z-average molecular weight defined by

$$\bar{M}_z = \frac{\sum_i w_i M_i^2}{\sum_i w_i M_i} \tag{42}$$

where w_i is the total weight of molecules of molecular weight M_i. However, as has been pointed out by Williams *et al.* (52), values of M_z are subject to a considerably higher degree of uncertainty as compared with M_w since they represent a higher moment of the distribution curve. Values of M_z are useful as a means of characterizing the polydispersity of the sample. For polydisperse substances $M_w < M_z$.

Table 11. Sedimentation equilibrium of ethyl hydroxyethyl cellulose fraction M12 in water.

r.p.m. (scale distance)	$c_0 = 0.247\%$					$c_0 = 0.165\%$				
	x	Z	c_i	$(M_i)_w$	$(M_i)_z$	x	Z	c_i	$(M_i)_w$	$(M_i)_z$
5,100 90	4.57	95	0.171	128,000	11,100	5.27	69	0.113	122,000	134,000
	4.62	97	0.191	116,000	11,000	5.32	80	0.128	124,000	136,000
	4.67	99	0.211	106,000	31,300	5.37	93	0.146	125,000	142,000
	4.72	103	0.232	99,000	59,900	5.42	109	0.167	127,000	128,000
	4.77	110	0.254	96,000	91,100	5.47	126	0.191	127,000	116,000
	4.82	121	0.277	96,000	104,700	5.52	144	0.218	126,000	133,000
	4.87	135	0.304	96,000	127,000	5.54	—	0.231	126,000	—
	4.92	—	0.333	99,000						
Average				101,000	68,400				126,000	130,000

Table 12. Sedimentation equilibrium of ethyl hydroxyethyl cellulose fraction M7 in water.

r.p.m. (scale distance)	$c_0 = 0.201\%$					$c_0 = 0.101\%$				
	x	Z	c_i	$(M_i)_w$	$(M_i)_z$	x	Z	c_i	$(M_i)_w$	$(M_i)_z$
5,150 120	5.16	50	0.138	103,000	—	5.78	31	0.063	122,000	—
	5.21	53	0.152	97,000	42,000	5.83	32	0.071	112,000	37,000
	5.26	56	0.166	93,000	49,000	5.88	37	0.080	114,000	129,000
	5.31	62	0.181	94,000	99,000	5.93	45	0.090	121,000	175,000
	5.36	69	0.198	95,000	111,000	5.98	56	0.103	130,000	189,000
	5.41	80	0.217	99,000	137,000	6.03	69	0.119	137,000	188,000
	5.46	93	0.240	103,000	146,000	6.08	87	0.139	147,000	208,000
	5.51	111	0.266	110,000	172,000	6.12	105	0.159	155,000	209,000
	5.54	125	0.284	116,000	198,000					
Average				100,000	125,000				132,000	177,000

In practice macromolecular solutions are never ideal in behavior and Schulz (53) and Wales *et al.* (54) have shown that a non-ideality correction may be made by means of the relation

$$\frac{1}{M_{w_i}} = \frac{1}{M_w} + B_e c_0 \tag{43}$$

where M_w is the true weight average molecular weight, M_{w_i} is the weight average molecular weight calculated by assuming ideal behavior ($B_e = 0$) and c_0 is the initial concentration. Thus, on plotting $1/M_{w_i}$ as a function of concentration a straight with slope B_e is obtained. The intercept is the reciprocal of the true weight average molecular weight.

Wales (54, 55) has shown that the non-ideality correction factor B_e is equal to two times the osmotic second virial coefficient as defined on page 532.

Table 13. Sedimentation equilibrium of ethyl hydroxyethyl cellulose fraction M5 in water.

r.p.m. (scale distance)	$c_0 = 0.242\%$					$c_0 = 0.121\%$				
	x	Z	c_i	$(M_i)_w$	$(M_i)_z$	x	Z	c_i	$(M_i)_w$	$(M_i)_z$
5,320 90	4.52	45	0.182	76,700	—	5.73	26	0.081	77,000	—
	4.57	48	0.194	76,000	64,000	5.78	28	0.088	75,600	62,000
	4.62	51	0.207	74,800	59,000	5.83	31	0.096	76,500	87,000
	4.67	56	0.221	76,100	96,000	5.88	38	0.105	84,700	180,000
	4.72	61	0.236	76,800	87,000	5.93	46	0.115	92,900	167,000
	4.77	68	0.253	79,000	112,000	5.98	56	0.128	100,900	171,000
	4.82	77	0.271	82,700	129,000	6.03	69	0.144	109,500	181,000
	4.87	94	0.294	92,100	211,000	6.08	90	0.164	124,400	231,000
	4.92	124	0.322	109,800	295,000	6.12	109	0.185	132,500	205,000
Average				82,800	153,000				100,000	178,000
5,270 90	4.52	28	0.187	63,000	—	5.73	16	0.086	61,000	—
	4.57	31	0.197	65,600	110,000	5.78	18	0.092	63,300	104,000
	4.62	35	0.208	69,500	133,000	5.83	21	0.099	67,900	139,000
	4.67	40	0.221	73,800	146,000	5.88	25	0.107	74,500	156,000
	4.72	44	0.236	75,300	99,000	5.93	29	0.116	79,000	131,000
	4.77	49	0.252	77,600	113,000	5.98	36	0.127	88,600	193,000
	4.82	56	0.270	82,000	142,000	6.03	47	0.141	103,500	238,000
	4.87	67	0.291	90,100	192,000	6.08	63	0.160	121,100	259,000
	4.92	77	0.316	94,400	146,000	6.12	77	0.179	131,500	219,000
Average				78,200	140,000				90,800	200,000
6,040 120	4.52	49	0.169	69,700	—	5.76	32	0.067	89,000	—
	4.37	55	0.182	71,800	96,000	5.81	42	0.077	100,000	191,000
	4.62	63	0.197	75,100	114,000	5.86	51	0.088	105,000	133,000
	4.67	70	0.215	75,600	85,000	5.91	61	0.103	107,000	122,000
	4.72	80	0.234	78,600	110,000	5.96	74	0.120	110,000	131,000
	4.77	89	0.256	79,200	85,000	6.01	90	0.141	113,000	131,000
	4.82	100	0.280	80,500	93,000	6.06	110	0.166	117,000	134,000
	4.87	112	0.308	81,100	89,000	6.11	136	0.197	120,000	140,000
	4.92	126	0.338	82,200	93,000	6.12	139	0.204	119,000	68,000
Average				78,000	95,000				111,000	134,000

Experimental and results

Sedimentation equilibrium measurements were carried out on samples M12, M7 and M5 using a Svedberg equilibrium ultracentrifuge with direct motor drive. For a description of experimental details the reader is referred to the monograph by Svedberg and Pedersen (35). Difficulties were encountered in the performance of the experiments due to the low sedimentation and diffusion constants. All experiments were made at a temperature of 20°C and in the concentration range between 0.1–0.3 per cent. Below 0.1 per cent the data obtained was unreliable while above 0.3 per cent impractically long times were required for the establishment of equilibrium. In one experiment where a concentration higher than 0.3 per cent was used, equilibrium was not established even after 2 ½ months. The results obtained are given in Tables 11, 12 and 13. Several other experiments which were spoilt by leak-

Table 14. Weight–average molecular weights for three fractions of ethyl hydroxyethyl cellulose in water.

Fraction No.	$\overline{M}_w$	$B \times 10^4$ mole cm^3 g^{-2}	
		From sedimentation	From osmotic pressure
M12	270,000	13	5.4
M7	200,000	12	7.6
M5	140,000	11	9.8

age are omitted. In the experiments reported here the time required for equilibrium was about two weeks.

Table 14 shows the true weight average molecular weights calculated according to equation (43) from the data in Tables 11, 12 and 13. It must be pointed out that the non-ideality correction has been made on the basis of measurements at two concentrations only and for this reason the final results should be considered with reservation. A justification for a linear extrapolation through two points is found in the fact that the osmotic pressure and light scattering measurements (to be described shortly) showed that the second virial coefficient was sufficient to characterise the data in the concentration range employed. Nevertheless, a comparison with the molecular weights obtained from sedimentation velocity and diffusion measurements (see Table 10) shows remarkably good agreement in all cases. It therefore seems justified to conclude that, in spite of the gross uncertainty in the non-ideality correction, the weight average molecular weights obtained in these experiments are substancially correct.

In connection with the Z-average molecular weights it will be noted that the results for fraction M12 are obviously incorrect. The accuracy of the calculation of $(M_i)_Z$ depends upon the difference between successive values of Z. Since the present system is such that these differences are low, the values of M_Z obtained cannot be relied upon. As pointed out by Svedberg and Pedersen (ref. 35, p. 315) small errors in the determination of Z will have a much larger effect on M_{Zx} than on M_{wx}.

In Table 14 a comparison is made between the second virial coefficient derived from the present experiments and that obtained directly from osmotic pressure measurements. It is seen that for samples M12 and M7 there is a considerable discrepancy for which no explanation can be offered at the present time.

(11) Light scattering

Introductory discussion

The subject of light scattering by solutions of macromolecules has been extensively reviewed by a number of authors (56–59). The following remarks are intended to summarise the theoretical basis of the method.

When a beam of unpolarised light of intensity I_0 enters a scattering medium, the intensity of the light scattered per unit volume exhibits an angular dependence given by

$$i_\theta = i_0 \, (1 + cos^2\theta)/2 = R_\theta \, I_0/r^2 \,. \qquad (44)$$

where θ is the scattering angle with reference to the forward direction of the indicent beam, i_0 is the intensity of the light scattered at 0°, r is the distance between the scattering solution and the detector, I_0 is the intensity of the incident light, and R_θ is known as the reduced intensity or Raleigh ratio at the angle θ. The turbidity, τ, of the system is defined as the relative decrease of the light intensity per unit length of the primary beam as a result of scattering:

$$\tau = -dI/I\,dl \tag{45}$$

and is related to R_θ and i_θ by the equation

$$\tau = (2\pi r^2/I_0)\int_0^\pi i_\theta \sin\theta\, d\theta = 2\pi \int_0^\pi R_\theta \sin\theta\, d\theta. \tag{46}$$

Zernike (60) has shown that the turbidity may be written as the sum of two terms, one due to density fluctuations (solvent scattering) and the other due to fluctuations in concentration. In practice the effect of the former is eliminated by subtracting the scattering due to the solvent from that of the solution.

Debye (61) has shown that in the case of molecules whose dimensions are much smaller than about one-twentieth of the wavelength, λ, of the incident light, the turbidity due to concentration fluctuations is related to the molecular weight of the solute by the equation

$$\frac{Hc}{\tau} = \frac{1}{M} + 2Bc \tag{47}$$

where c is the concentration of polymer in solution in gm/cc, M the molecular weight of the polymer, and B the second osmotic virial coefficient (see page 532). H is a constant given by

$$H = 32\pi^3 n_0^2 \left(\frac{n-n_0}{c}\right)^2 \Big/ 3\lambda^4 N \tag{48}$$

where N is Avogadro's number, λ the wavelength in vacuo of the light used, n and n_0 are the refractive indices of the solute and solvent respectively.

Introducing instead of H, a new constant K defined by the equation

$$K = 2\pi^2 n^2 (dn/dc)^2/\lambda^4 N, \tag{49}$$

equation (47) can be expressed in the alternate form

$$\frac{Kc}{R_{90}} = \frac{1}{M} + 2Bc. \tag{50}$$

Molecular weights are obtained by extrapolation of a plot of Hc/τ or Kc/R_{90} against c to infinite dilution. If the measurements have not been made at too high concentration the extrapolation is linear and the intercept at $c = 0$ is equal to the reciprocal of the molecular weight.

There are, however, many macromolecules having dimensions comparable to the wavelength of the incident light. As a result of the phase shifts encountered by rays scattered from different parts of the same molecule, interference effects are produced

and lead to an unsymmetrical scattering which can be characterized by a dissymetry coefficient, z_{45}, equal to the ratio of the light scattered at 45° to the incident beam to that at 135°.

Zimm (62) has shown that in the case of large molecules equation 50 can be rewritten as

$$\frac{Kc}{R_\theta} = \frac{1}{MP(\theta)} + 2Bc \qquad (0 < \theta < 180) \tag{51}$$

where $P(\theta)$ is a particle scattering factor which corrects for the effects of internal interference. $P(\theta)$ is related to the form and dimensions of the solute molecules by the following expressions (63–66)

$$\text{sphere, } P(\theta) = \left[\frac{3}{x^3}(\sin x - x\cos x)\right]^2;\ x = \frac{ksD}{2} \tag{52}$$

$$\text{rod, } P(\theta) = \frac{1}{x}\int_0^{2x} \frac{\sin\omega}{\omega} d\omega - \left(\frac{\sin x}{x}\right)^2;\ x = \frac{ksL}{2} \tag{53}$$

$$\text{Gaussian coil, } P(\theta) = \frac{2}{x^2}[e^{-x} - (1-x)];\ x = \frac{k^2 s^2 R^2}{6} \tag{54}$$

where $k = 2\pi/\lambda'$, λ' being the wavelength of light in the solution, $s = 2\sin\theta/2$, $D =$ diameter of sphere, $L =$ length of the rod and $R =$ root-mean-square of the distance between ends of the random coil.

In all cases the function $P(\theta)$ tends towards unity as θ tends towards zero, there being no intraparticle interference in the direction of the incident beam.

It is sometimes more convenient to express $P(\theta)$ as a series expansion in θ. Equation 53 may thus be written as (ref. 59)

$$\frac{1}{P(\theta)} = 1 + \frac{n^2}{9} + \frac{7n^4}{2025} + \cdots \tag{55}$$

where $n = (2\pi L/\lambda)\sin\theta/2$ and equation (54) as (ref. 59):

$$\frac{1}{P(\theta)} = 1 + \frac{n}{3} + n^2/36 + \cdots \tag{56}$$

where $n = 8/3\pi^2(R/\lambda)^2 \sin^2\theta/2$.

In general, two methods have been used for the treatment of light scattering data. In the dissymmetry method the intensity of the scattered light is measured at two angles which are supplementary. The dissymmetry thus found may be used to calculate the particle size for any particle shape assumed, and the correction $P(\theta)$ which is to be applied to obtain the true molecular weight. Alternatively the intensity is measured at various angles and Kc/R_θ is plotted against concentration. The slope determines the second virial coefficient, and the intercept with the Kc/R_θ axis gives $M/P(\theta)$ which yields the reciprocal of the molecular weight on extrapolation to zero angle. Both extrapolations may conveniently be carried out in a

single graph by the Zimm method (67). Here Kc/R_θ is plotted against $sin^2\,\theta/2 + k\,c$, where k is an arbitrary constant chosen to spread out the data. Thus treated, the data form a grid in which extrapolated points are joined into two lines that should meet at the same intercept of Kc/R_0 at zero concentration. The reciprocal of the intercept is equal to the molecular weight. The value of B is obtained from the slope of the zero angle line, while the dimension can be calculated from the ratio of the slope of the zero angle line to the intercept, viz.

$$(\bar{R}^2)^{\frac{1}{2}} = \frac{9\,\lambda'^2\ \text{(limiting slope)}}{8\,\pi^2\,(K\,c/R_\theta)_{c=0}} \tag{57}$$

where λ' is the wavelength of the incident light in the solution. The molecular dimension may also be expressed in terms of the so-called radius of gyration, or root-mean-square radius from the centre of mass of the particle. It is related to the characteristic dimension by the expressions

sphere: $$(\bar{R}_g^2) = 3\,D^2/20, \tag{58}$$

rod: $$(\bar{R}_g^2) = L^2/12, \tag{59}$$

coil: $$(\bar{R}_g^2) = R^2/6. \tag{60}$$

Information about the shape of the particle may in principle be obtained by the comparison of the observed and calculated angular scattering functions.

In the case of a polydisperse system the light scattering method gives a weight-average molecular weight and a z-average molecular dimension; i.e. the dimension of a particle having a molecular weight, M_z. The form of the $1/P(\theta)$ function depends not only on the molecular size but also on the polydispersity of the sample (67). For the special case where the distribution corresponds to $M_z : M_w : M_n :: 3:2:1$ the plot of $1/P(\theta)$ against $sin^2\,\theta/2$ is linear and there are no difficulties in interpretation. When the molecular size is sufficiently large and the system polydisperse, the precise determination of the angular distribution of the scattered light can give M_n, M_z, M_w and the corresponding average dimensions (68).

Experimental methods and results

The measurements were made with an instrument constructed and calibrated by Dr. A. Bengtsson of this Institute. Details will be published elsewhere. The design is similar in many respects to others previously described (cf. e.g. ref. 67). It was operated on the "null" principle, i.e., the scattered light observed by a photomultiplier detector was balanced by means of an electronic bridge circuit against a portion of the incident beam which was diverted by a mirror system to a photoelectric tube. An electronic voltmeter was used to observe the balance of the opposed and amplified 100 cycle signals from the photomultiplier detector and the incident light monitor. The light source was a Philips Philora H 500 medium-pressure mercury lamp. The 5460 and 4358 Å lines were isolated by means of Zeiss filter combinations. Unpolarised incident light was used throughout.

In carrying out light scattering measurements it is important that the intensity of the light scattered from the solutions under study be directly compared with

that of a working standard material which has itself been calibrated in absolute terms. The absolute calibration was based upon reflectivity measurements of a MgO surface. Such a surface does not act as an ideal diffusor; there being always at least a small fraction of the light which undergoes spectral reflection, and a small correction was applied to take care of the non-ideality of the diffusor. The reflectivity of the diffusor was 0.97 at a wave length of 4358 Å. This absolute calibration was checked by measuring the excess turbidity of a 0.5 per cent solution of Dow Styron in toluene. The value obtained was 3.50×10^{-3} cm^{-1} at 4358 Å as compared with 3.51×10^{-3} cm^{-1} reported by Brice *et al.* (69). A neutral filter (optical density about 10^{-5}) placed in the primary beam and measured at zero angle served as a working standard.

Because of the strong dependence of the intensity of scattering on the volume of the particles, it is extremely important in light scattering measurements to eliminate dust and other foreign impurities which scatter a considerable amount of light even when present in relatively small concentrations. As a result of the great dissymmetry of the radiation envelope of dust particles, even greater care is required when angular dependence measurements are to be made. It has long been known that the optical clarification of aqueous solutions poses special problems and in this respect great difficulties were encountered in the present investigation. In initial experiments stock solutions were first cleaned by centrifuging for one hour at 30,000 r.p.m. in the large rotor of the Spinco preparative ultracentrifuge. The amount of material centrifuged out, as a gel-like deposit on the bottom of the cell, was in all cases very small and no change could be detected in the concentration of the solution. The solutions were carefully syphoned from the centrifuge tubes and then filtered through a Jena-G 5 filter directly into the light scattering cell. Even after this treatment abnormally high dissymmetries ($z_{45} = 2 - 4$) were observed for all fractions. Careful visual examination of the low angle scattering in green light with the aid of a lens revealed the presence of a very small amount of motes. This, however, could not account for the high dissymmetries observed.

Working on the hypothesis that the difficulties were due to undispersed particles of very high molecular weight, a number of experiments were carried out in an attempt to remove them.

1. Aqueous solutions were centrifuged at 30,000 r.p.m. for thirty-six hours. The middle portion of the solution in each tube was removed by careful syphoning and its dissymmetry measured.

2. The polymer was dissolved in 0.5*N* sodium hydroxide and the dissymmetry was measured. Higher concentrations of sodium hydroxide could not be used since the solutions thus obtained were highly turbid.

3. If aggregation due to the formation of random hydrogen bonds is present in polymer solutions, it should be dispersed by the addition of a hydrogen-bond breaking agent such as urea. This has been demonstrated by Alexander and Stacey (71) in the case of polyvinyl alcohol. In the present case such a type of aggregation seemed likely to occur, in view of the many hydroxyl groups in the polymer. The light scattering was measured in 3 and 6 molar urea solutions.

4. Solutions were heated to a temperature of 50°C for several hours and the dissymmetry was measured at this temperature. It was expected that the increased thermal motion might be sufficient to break up any aggregates present. Higher temperatures could not be used since, as pointed out before, gelation or flocculation would result.

5. Scattering measurements were made on solutions at a temperature of about 5°C. Prior to the measurements the solutions had been maintained at that temperature for several hours.

Since the solutions exhibit a negative temperature coefficient of viscosity, aggregates due to partial substitution of the cellulose chains might become molecularly dispersed at these low temperatures.

6. Dissymetries were measured on solutions before and after freezing (see page 526).

7. Solutions were exposed to ultrasonic vibrations at a frequency of 600 *Kc* for about thirty minutes. Higher frequencies were not used because of the danger of degradation.

8. In the fractionation studies it had been found that large amounts of acetone could be added to the aqueous solutions of the polymer without causing any appreciable precipitation. Nevertheless, it was felt that aggregated material would perhaps be precipitated under such conditions. To one volume of aqueous polymer solution three volumes of acetone were added. After allowing the solution to stand for twenty-four hours it was centrifuged for one hour at 30,000 r.p.m. The clear solution thus obtained was poured into excess acetone in order to effect quantitative coagulation of the polymer which then dried by methods previously described. The polymer was then redissolved in water and the scattering was measured.

In all of the above experiments high dissymmetries were still obtained regardless of the fraction used.

It was finally found that there was a considerable decrease in dissymmetry after filtration through membrane filters (Membranfilter Gesellschaft, Göttingen, Germany). These filters are supplied in four grades; large, medium, fine and ultrafine having pore sizes of 0.75–3.0, 0.5–0.75, 0.2–0.5 and <0.2–microns respectively. Only the large size could be used since the others became completely clogged. Even for the large size concentrated solutions ($c > 0.3$ per cent) could not be filtered for the same reason.

The solutions were first cleaned by centrifugation as described above and then filtered under 1–2 kg/cm nitrogen pressure through the membrane filter clamped in a Seitz holder. Provided the solutions were sufficiently dilute no change in concentration could be detected but in all cases concentration determinations were made on filtered solutions. Dissymmetry-free water ($z_{45} = 1$) used for dilutions was obtained by filtering laboratory distilled water through large or medium size filters. Filtrations were made directly into the light scattering cell, a new filter being used for each solution. By the use of these membrane filters fewer precautions were needed in cleaning transfer pipettes and dilution flasks since dust left behind after the usual cleaning procedures could be removed by filtration.

The green line of mercury (5460 Å) was used in all the measurements after it had been established that the blue line (4358 Å) gave the same value of Kc/R_θ, showing thereby that fluorescence was negligible.

Scattering measurements were made on the solvent and a series of each sample prepared by volume dilution of a clarified stock solution, each solution being filtered individually. Measurements were only made when careful visual examination at low angles did not reveal any motes.

The dissymmetry of scattered light was rather large in most cases. Under such circumstances the extrapolation method is to be preferred since it is independent of assumptions of particle shape, makes use of more data, and yields more precise values of the molecular size and weight. For the angular intensity measurements a cylindrical cell having flat entrance and exit windows for the primary beam was used. Intensities measured at 7–8 angles covering the range from 40 to 135° were corrected for the following effects. (*a*) As unpolarised incident light was used, the scattered light contained a horizontal component proportional to $\cos^2 \theta$. Intensities

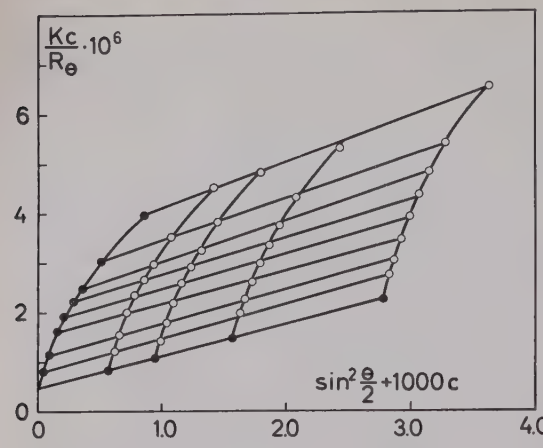

Fig. 18. Zimm plot for ethyl hydroxyethyl cellulose fraction M7 in water. The solutions were cleaned by high speed centrifugation followed by filtration through an ultrafine glass filter. The intercept $(Kc/R_\theta)_{c\to 0}$ corresponds to a molecular weight of 2.08×10^6.

were therefore normalised by multiplication with the factor $(1 + cos^2\ \theta)^{-1}$. (*b*) The volume of the scattering solution "viewed" by the receiver varies with the angle. This may be approximately corrected by multiplying the measured intensity by sin θ. (*c*) When the scattered light is incompletely polarised there may be a small contribution to the measured intensity arising from fluctuations in orientation of the solute. The application of this correction requires a knowledge of the depolarization $\varrho = H_u/V_u$, where H_u and V_u denote the intensities of the horizontal and vertical components of the scattered light when the incident light is unpolarised. The depolarization was measured by means of a polaroid placed in the scattered beam in the 90° position. The average depolarization ϱ for all fractions was found to be 0.02 and the molecular weight was multiplied by the Cabannes factor $(6–7\varrho)/(6 + 6\varrho)$. (*d*) The scattered light undergoes refraction at the cell wall. The correction for this effect was accomplished in the manner indicated by Hermans and Levinson (70) who have shown that the correction factor is proportional to the square of the refractive index of the solution, irrespective of the shape of the scattering cell, provided the receiver does not see past the edges of the beam. The geometrical arrangement of the apparatus was such that this requirement was met. (*e*) Intensities of the solvent were subtracted from those of the solution.

Reciprocal intensity plots were made for all fractions. Molecular weights were computed from intercepts of the bilinear extrapolation on the ordinate and molecular sizes were calculated according to equation 57. Fig. 18 shows a typical Zimm plot obtained when the solutions were filtered through glass filters. It indicates the presence of very large particles (weight average M_w, 2.08×10^6) but it is clear from the curvature in the angular scattering plots that the mixture is very polydisperse. The result obtained when a portion of the same solution was filtered under pressure through membrane filters is shown in Fig. 19. The marked change in the shape of the reciprocal scattering envelope and the considerable decrease in molecular weight $(M_w = 0.4 \times 10^6)$ indicates that some of the large particulate matter had been removed by the membrane filtration. In fact, the linearity of the angular scattering curves leads one to believe that the solutions are free of all foreign matter. This plot is typical of that obtained for the other three fractions. In all cases the dissymmetry showed a very slight linear increase with decrease in concentration.

The results obtained are collected in Table 15.

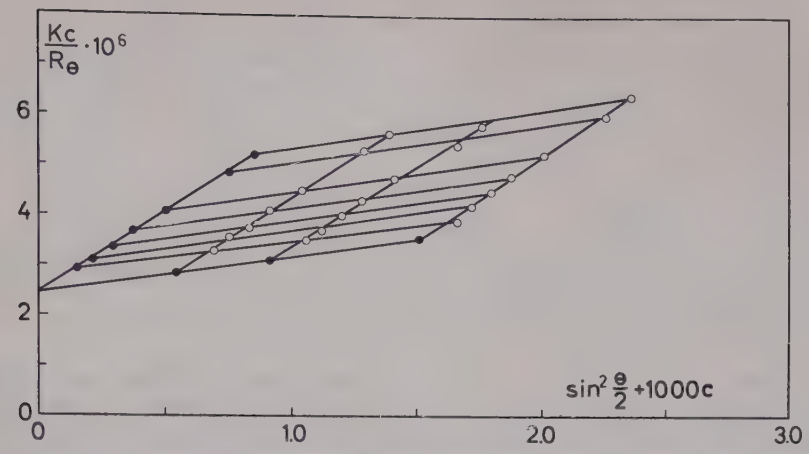

Fig. 19. Zimm plot for ethyl hydroxyethyl cellulose fraction M7 in water. The solutions were cleaned by high speed centrifugation followed by filtration through cellulose membranes. The intercept $(Kc/R_0)_{c\to 0}$ corresponds to a molecular weight of 4.0×10^5.

Table 15. Molecular weights and dimensions of ethyl hydroxyethyl cellulose in water at 20°C as determined by light scattering.

Fraction No.	$(z_{45})_{c\to 0}$	$B \times 10^4$ mol. cm³ g^{-2}	R_z [Å]	$M_w \times 10^{-3}$ By Zimm method	$M_w \times 10^{-3}$ from $(z_{45})_{c\to 0}$[1]
12	2.0	1.5	1870	570	530
7	1.80	3.6	1630	400	410
5	1.70	1.7	1370	250	250
3	1.45	5.3	1270	160	170

[1] Assuming coil model.

Part 2

General discussion

(1) Molecular weights and polydispersity of the fractions

In Table 16 the molecular weights obtained by the different methods and the corresponding degrees of polymerization are assembled for purposes of ready comparison. It is immediately evident that the values from light scattering are about twice as great as those from sedimentation–diffusion and sedimentation equilibrium. The results from light scattering and sedimentation equilibrium should be the same since both methods give a weight average. There are three possible explanations for the discrepancy. (*a*) The light scattering apparatus is faulty and leads to a systematic error in the results. This possibility may be dismissed in view of the fact that the correct molecular weight was obtained for an International Polystyrene sample (72). (*b*) As a single stage fractionation was used, the samples may be very broad

Table 16. Molecular weights, degrees of polymerization and

Fraction No.	$M_n \times 10^{-3}$	$M_{ww} \times 10^{-3}$	$(M_w)_{sed} \times 10^{-3}$	$M_z \times 10^{-3}$ (1)	$(M_w)_{L.S.} \times 10^{-3}$
M12	176	310	270	480	570
M7	128	200	200	310	400
M5	77.6	140	140	200	250
M3	52(1)	92	90	160	160

(1) deduced from relation between $[\eta]$ and $\bar{M}$.
(2) calculated from M_n and $(M_w)_{sed}$; assuming Kraemer-Lansing distribution.

and may have a distribution showing a long high molecular weight tail. (*c*) Each fraction contains a wide spectrum of high molecular aggregates. Although the greater part of these are removed by the method of cleaning the solutions, a very small portion persists and affects the light scattering results.

Before discussing these two latter possibilities we consider briefly the question of whether the light scattering data has been correctly interpreted.

Polydisperse systems of sufficiently high molecular weight may exhibit curvature of the reciprocal scattering envelopes (67). According to Benoit (68) two different molecular weight averages may then be obtained as follows:

$$\bar{M}_w = 1/(Kc/R_0)_{c=0},$$
$$\bar{M}_n = 1/(2 \times \text{intercept of asymptote}).$$

Thus it may be that in the present cases the measurements may have been made on the asymptote and a possible curvature at lower angles has been missed. If this is true then the molecular weights obtained are in reality twice the number-average molecular weight. Comparison with the osmotic pressure data reveals, however, that such an interpretation is impossible. This is further shown by the fact that the M_w values calculated by the Zimm and dissymmetry methods are in good agreement.

We consider next the question of the breadth of the distributions implied by the light scattering and osmotic molecular weights.

Perhaps the simplest means of expressing molecular heterogeneity is to compare the different average molecular weights $\bar{M}_n$, $\bar{M}_w$, $\bar{M}_z$. As pointed out before, in a monodisperse system all the averages will have the same value and from a qualitative standpoint it may be said that the greater the spread in the average molecular weights, the greater is the polydispersity. The unique evaluation of molecular size distributions in polymer systems is a very complicated problem. A method which has generally been used is to fit an assumed parametric function to the observed average molecular weights (cf. e.g. 38, 73). Of the several model distributions available it is convenient to choose the single-peaked Lansing–Kraemer logarithmic exponential function (74). It makes no difference if this does not really represent the actual distribution since it is only being used here for characterizing the polydispersity. The weight distribution is then defined as

$$f(M)\,dM = dw = \frac{w}{\bar{M}_n \beta \sqrt{\pi}} \exp\left(-\frac{1}{\beta} \ln M/M_0\right)^2 dM \qquad (61)$$

polydispersity for fractions of ethyl hydroxyethyl cellelose.

$M_v \times 10^{-3}$	Z_n	Z_{ww}	$(Z_w)_{sed}$	$(Z_w)_{L.S.}$	$(M_w)_{sed}/M_n$
280	840	1480	1300	2900	1.5
190	610	960	940	2000	1.5
133	370	670	660	1200	1.8
86	250(1)	430	430(1)	800	1.7

where dw is the weight of polymer having a molecular weight between M and $M+dM$; w is the total weight of polymer (usually normalized to one), M_0 is the molecular weight at the maximum of the weight distribution curve, $\bar{M}_n$ is the number average molecular weight and β is a non-uniformity coefficient, equal to zero for a monodisperse sample. Equation (61) may also be expressed in integral form by plotting the function $F(M)$ as a function of M, where

$$F(M) = \int_0^M f(M)\, dM.$$

For polydisperse systems with the above distribution the following relationships are valid

$$\bar{M}_z/\bar{M}_w = \bar{M}_w/\bar{M}_n = e^{0.5\beta^2} \tag{62}$$

$$M_p/\bar{M}_w = e^{1.25\beta^2} \tag{63}$$

$$M_0 = M_p\, e^{0.5\beta^2} \tag{64}$$

Typical distribution curves constructed on the basis of the above relations using $\bar{M}_n$ from osmotic pressure and $\bar{M}_w$ from light scattering are shown in Fig. 20. For the sample in question (M5) the following characteristic constants were found $M_0 = 43{,}000$, $\beta = 1.5$. About 15 per cent of the material has a degree of polymerization greater than 2500. From our knowledge of the molecular weight of cellulose itself and taking into consideration the degradation which is known to occur during the preparation of this derivative, such a result seems highly unlikely. This is even more apparent when it is realised that this is one of the low molecular weight fractions.

Independent support for the opinion that the fractions do not possess the broad distribution indicated by the light scattering results was derived from two sources, namely from an analysis of the sedimentation velocity diagrams and by a comparison of polydispersity indices derived from sedimentation equilibrium and osmotic pressure on the one hand and the diffusion measurements on the other.

Several methods are available for the sedimentation analysis of polydisperse macromolecular systems (38, 75). The method used in the present case was developed by Eriksson (76) and successfully applied to a study of polydispersity in polymethylacrylate. Very briefly, the method is as follows. The integral distribution of sedimentation constants is determined at various points on the sedimentation curve.

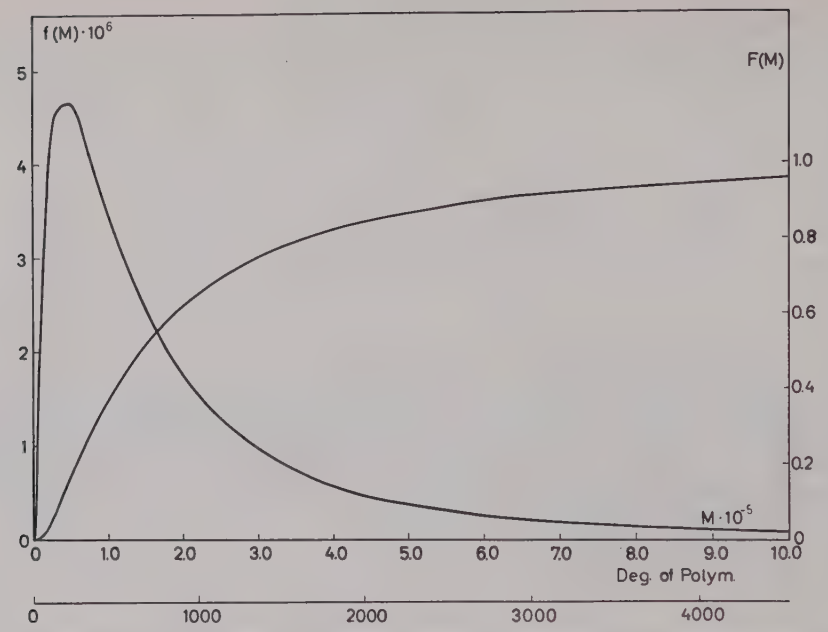

Fig. 20. Differential and integral distribution curves as calculated from the osmotic and light scattering molecular weights for fraction M5.

This apparent distribution is then extrapolated to infinite time and infinite dilution in order to eliminate the effects of diffusion and concentration. Fig. 21 shows the distribution of sedimentation constants for the fraction considered above. On the basis of the results from sedimentation–diffusion and sedimentation–equilibrium the scale on the abscissa corresponds to a molecular weight range of 90,000 to 300,000. Thus all the molecules in the sample have a degree of polymerization less than 1500.

Gralén (37) has shown that it is possible to calculate the Lansing–Kraemer non-uniformity coefficient β from diffusion measurements.

Assuming a logarithmic distribution of diffusion constants, viz.,

$$dc = K_D\, e^{-y^2}\, dD \tag{65}$$

where $y = (1/\gamma)\ log\ (D/D_1)$, the diffusion constants as derived by the area and moment methods are related by the equation

$$D_A/D_1 = D_m/D_A = e^{3\gamma^2/8}. \tag{66}$$

Here K_D is a constant, γ is the distribution coefficient for the diffusion constants and D_1 is the diffusion constant at the maximum point of the distribution curve. If

$$M = \frac{\text{const}}{D_a} \quad \text{and} \quad M = \text{const}\ s^b$$

then
$$(a-1)\ (b-1) = 1 \tag{67}$$

and
$$\beta = \gamma\, a. \tag{68}$$

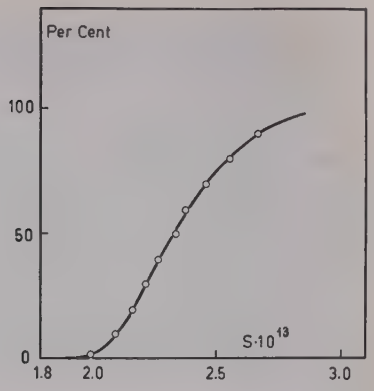

Fig. 21. Percentage of material with sedimentation constants less than S (fraction M5).

In Table 17 it is seen that the values of β calculated from light scattering–osmotic pressure are considerably higher than those derived from sedimentation equilibrium –osmotic pressure and diffusion. The values obtained from the two latter methods are in good agreement.

We turn now to the question of aggregation. Over the concentration range (0–0.3 per cent) at which the different measurements were normally made there was no evidence of a second component in the usual sedimentation diagrams; and observations during the acceleration period did not reveal any fast sedimenting molecular species. With the aid of a Schlieren optical system some observations made on 2 per cent solutions (not cleaned by preparative centrifugation) showed a small peak which sedimented within five minutes after the centrifuge was turned on. During the first 15–20 minutes of the acceleration period there was a a considerable irregularity of the base lines which, however, later disappeared. Solutions which had been cleaned in the Spinco preparative ultracentrifuge did not show these effects.

From the preceding discussion the conclusion may be drawn that all the samples contain a small amount of aggregated material. A portion of this is removed when the solutions are cleaned in the Spinco preparative centrifuge. The amount which remains behind is too small to be detected in sedimentation velocity diagrams, if not centrifuged out already during the acceleration period. Thus molecular weights calculated from sedimentation data are not affected by the presence of such material.

Table 17. Values of the the Lansing-Kraemer non-uniformity coefficient as derived from the different experimental methods used.

Fraction No.	β		
	Light-scattering + osmotic pressure	Sedimentation equilibrium + osmotic pressure	Diffusion
M12	1.5	1.0	1.3
M7	1.5	0.94	1.08
M5	1.5	1.08	1.08
M3	1.5	1.07	1.08

The discrepancy between the molecular weights obtained from sedimentation–diffusion and sedimentation–equilibrium on the one hand and light scattering on the other, is due to a small amount of aggregated material present in the light scattering solutions in spite of the methods of clarification.

It is obvious that on a number basis the amount of aggregated material present in the solutions is negligible and hence would have no effect on the number average molecular weight. Several workers (cf. e.g. refs. 71, 77) have shown that aggregation has little or no effect upon viscosity even when present in a considerable degree. The same conclusion might be drawn in the present case since the same intrinsic viscosity was found for solutions cleaned by filtration through coarse glass filters (Jena G3) and by high speed centrifugation.

Finally, we consider briefly the question of the origin of the aggregates. It is clear from the various attempts at dispersion that extremely strong chemical valence forces are involved. As such forces are present in cellulose itself it seems most probable that the aggregation is due to the uneven distribution of substituents along the cellulose chains. An analogous situation appears to exist in the case of cellulose xanthate (78) and sodium carboxymethyl cellulose (79) and may be interpreted, following Höppler (81) and Ott (80), in terms of the pecularities of the etherification reaction of cellulose. In the preparation of alkali cellulose and its subsequent conversion to ethyl hydroxyethyl cellulose a uniform distribution of substituents along the cellulose chain would not be expected, since accessible regions in the amorphous portions of the cellulose and on the periphery of the crystalline regions would react more rapidly than the interior of the highly crystalline portion. Upon dispersing the ethyl hydroxyethyl cellulose in water, while most of it dissolves molecularly there still remains a small percentage of molecules which are held together by the crystalline remnants from the original cellulose. That this view is essentially correct is supported by Fig. 22 which shows a number of photomicrographs of the gel-like deposit isolated from 2 per cent solutions of ethyl hydroxyethyl cellulose by high speed centrifugation. The pictures were obtained with the aid of phase contrast microscopy. In view of what has been said above, there is every reason to believe that the particles seen here merely represent the upper range of a wide spectrum of large particulate matter. The pictures reveal a number of interesting factors in connection with the preparation of alkali cellulose and the morphology of cellulose fibers. Further discussion of the matter is, however, beyond the scope of the present work.

This investigation therefore emphasises the fact, perhaps well known but mostly neglected, that the characterization of high molecular materials and cellulose derivatives in particular, solely on the basis of light scattering and viscosity measurements is not only unwise but decidedly hazardous.

As pointed out before, the weight average molecular weights from sedimentation equilibrium measurements are in good agreement with the weight–weight average from sedimentation–diffusion. It is known that $M_n < M_{ww} < M_w$, and for certain special theoretical distributions Jullander (38) and Singer (82) have shown that M_{ww} should be closer to the number than to the weight average. However, since in actual practice M_{ww} is often found to lie rather close to M_w (38, 83), the agreement obtained here is not unusual, and it seems justified to take the M_{ww} values as a very close approximation to M_w.

Values of M_w/M_n, used as measure of polydispersity, are given in Table 16. Values of M_z calculated on the assumption that the fractions have a distribution

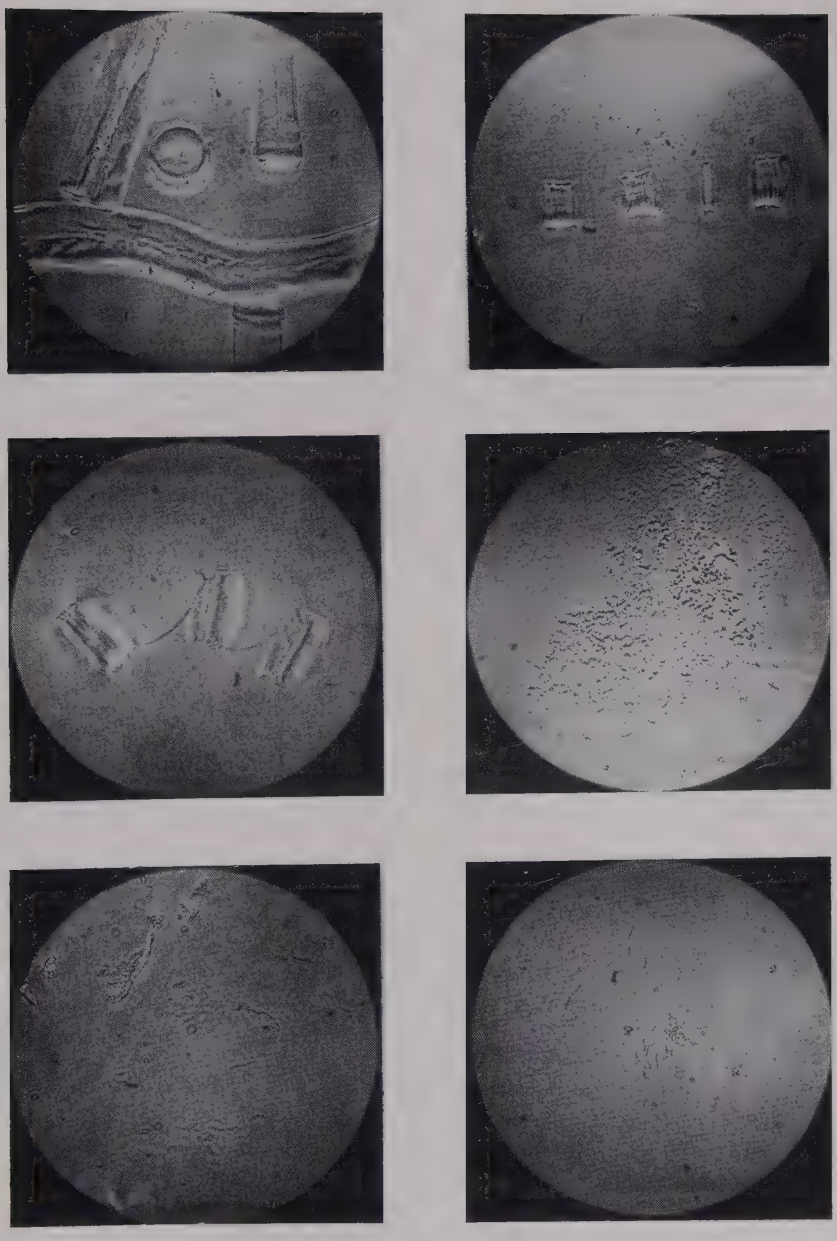

Fig. 22. Photomicrographs of the gel fraction isolated from 2 per cent solutions of ethyl hydroxyethyl cellulose. Fiber fragments of various sizes and state of swelling are seen.
(Magnification 320 ×.)

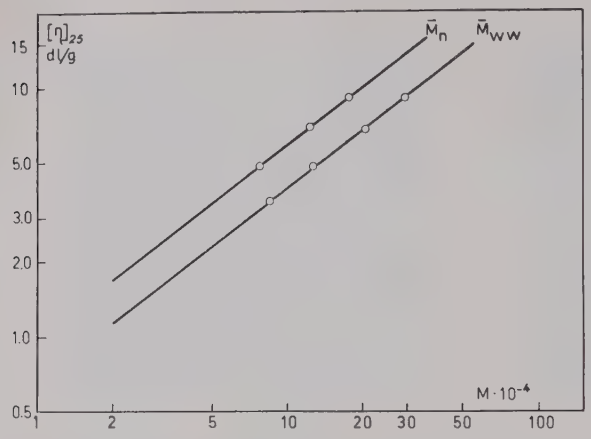

Fig. 23. Double logarithmic plots showing the dependence of intrinsic viscosity at 25°C on the number-average (M_n) and weight-weight (M_{ww}) average molecular weights for ethyl hydroxyethyl cellulose in water.

of the Lansing-Kraemer form are also given in the same Table. It is evident that all the fractions investigated are rather polydisperse. This, however. is precisely what one expects since only a single stage fractionation was used. It is expected that sharper fractions would have been obtained by refractionation but the difficult and time consuming nature of the method made such a course impractical. Furthermore, it is doubtful whether refractionation by this method would provide the sharpness necessary for more precise determinations of the molecular parameters (see also page 522).

(2) Molecular weight dependence of $[\eta]$, s and D

According to Staudinger (84), in solutions of threadlike molecules the intrinsic viscosity is proportional to the molecular weight. More recent investigations have, however, shown that this is a special case of the more general relation

$$[\eta] = KM^a$$

where K is a constant independent of molecular weight. Several theoretical developments, to be discussed shortly, indicate that the exponent a may have values lying between the extremes of 0 and 2 depending upon the flexibility of the polymer chains but not on the molecular weight. Three special cases are worthy of note. When a approaches the limiting value of 2 it implies that the molecules have a rod-like configuration. For free draining random coils $a = 1$, and $a = 0.5$ corresponds to a compact solvent immobilizing coil.

Fig. 23 shows a double logarithmic plot of $[\eta]_{25}$ against M_n and M_{ww}. The relation between intrinsic viscosity and molecular weight can be expressed by the equation

$$[\eta]_{25} = 3.7 \times 10^{-4}\, \bar{M}_{ww}^{0.8}. \tag{69}$$

Based on number average values the relation is given by

$$[\eta]_{25} = 4.70 \times 10^{-4}\, \bar{M}_n^{0.8}. \tag{70}$$

Relations (69) and (70) are reliable only for fractions having relatively narrow molecular weight distributions. In the comparison of samples with broad molecular

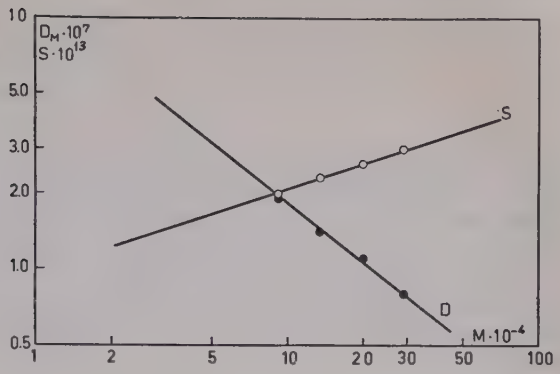

Fig. 24. Log-log plots of D_m and S against M_{ww} for fractions of ethyl hydroxyethyl cellulose in water.

weight distributions it is more correct to use the relationship between the intrinsic viscosity $[\eta]$ and the viscosity average molecular weight (85) defined by

$$M_v = \left[\frac{\sum_i n_i M_i^{1+a}}{\sum_i n_i M_i}\right]^{1/a}. \tag{71}$$

Flory (85) has indicated that when $0 < a < 1$,

$$M_n < M_v < M_w.$$

In order to calculate M_v it is necessary to make some assumption about the distribution. For the Lansing-Kraemer distribution (74) the following relation is valid

$$M_v = M_0 \exp\left\{\frac{\beta^2}{2}(1 + a/2)\right\} \tag{72}$$

where the symbols have the previously mentioned significance. On the other hand the "most probable distribution" (86) is characterized by

$$\frac{M_v}{M_w} = \frac{[(1+a)\,\Gamma(1+a)]^{1/a}}{2} \tag{73}$$

where $\Gamma(1+a)$ is the gamma function of $(1+a)$.

Taking the value of the exponent a to be 0.8, values of M_v were calculated for the four fractions. Almost identical values were obtained from equations (72) and

Table 18. Dependence of the sedimentation and diffusion constants on molecular weight for different molecular models.

	Compact coil	Free draining coil
Diffusion constant	$D \sim M^{-1/3}$	$D \sim M^{-1}$
Sed. constant	$s \sim M^{-1/3}$	$s \sim M^{0}$

(73). The results are given in Table 16. The best straight line in the double logarithmic plot of M_v against $[\eta]$ is represented by the equation

$$[\eta]_{25} = 3.98 \times 10^{-4}\, M_v^{0.8}. \tag{74}$$

While it is possible that neither of these functions gives a really true description of the actual distribution in the fractions, the fact that the same relation is obtained when two different model distributions are used suggests that equation (74) is relatively insensitive to the distribution assumed and strongly supports its reliability.

Relations analogous to equations (69) and (70) exist between the molecular weight and the sedimentation and diffusion constants. Fig. 24 shows double logarithmic plots of s and D_M against molecular weight. The straight lines correspond to the relations

$$s = 3.1 \times 10^{-2}\, M^{0.36}, \tag{75}$$

$$D_M = 10^4\, M^{-0.7}. \tag{76}$$

The exponent of the molecular weight has a characteristic value depending upon the shape of the molecules. Table 18 shows the dependence of the sedimentation and diffusion constants on molecular weight for the extreme cases of free draining and solvent–immobilizing coils (87).

From the exponent of the molecular weight in equations 69, 70, 75 and 76 the conclusion may be drawn that over the range of molecular weights studied, the molecule of ethyl hydroxyethyl cellulose has a form which lies between that of a free draining and solvent–immobilizing coil. Further information about molecular size and shape will be given in succeeding paragraphs.

(3) Relation of hydrodynamic behavior to molecular configuration

Several theories of linear polymers of random coil structure have been developed to account for the hydrodynamic interaction of the monomer units of the polymer and for the partial immobilization of solvent within the coil. These theories permit, at least in principle, the calculation of parameters which belong to well defined models and give a better picture of the molecular structure or behavior. Although the functional relationships arising from the several treatments are strictly applicable only to monodisperse systems, it is nevertheless of interest to consider the present results in terms of certain of these theories, in particular those of Kuhn and Kuhn, Debye and Bueche, Kirkwood and Risemann and Flory and Fox.

The theory of Kuhn and Kuhn (88) is based upon the model of a statistically coiled string of beads. From experiments on large scale wire models they deduced the intramolecular hydrodynamic interaction and arrived at the following formulae

$$[\eta] = \frac{N A_m b_m^2}{M_0} \frac{0.43\, Z}{-1.6 + 2.3 \log_{10} (A_m/d_h) + (b_m Z/A_m)^{\frac{1}{2}}} \tag{77}$$

$$s = a_1 + b_1 \sqrt{Z} \tag{78}$$

$$D = (a_2 + b_2 \sqrt{Z})\, Z^{-1} \tag{79}$$

where

$$a_1 = \frac{M_0}{N b_m} \frac{1 - V\varrho}{\eta_0} \left[-0.03 + 0.16 \log_{10} \left(\frac{A_m}{d_h} \right) \right] \tag{80}$$

$$b_1 = \frac{M_0}{N b_m} \frac{1 - V\varrho}{\eta_0} 0.136 \left(\frac{b_m}{A_m} \right)^{\frac{1}{2}} \tag{81}$$

$$a_2 = \frac{kT}{\eta_0 b_m} \left[-0.03 + 0.16 \log_{10} \left(\frac{A_m}{d_h} \right) \right] \tag{82}$$

$$b_2 = \frac{kT}{\eta_0 b_m} 0.136 \left(\frac{b_m}{A_m} \right)^{\frac{1}{2}} \tag{83}$$

for the intrinsic viscosity, sedimentation and diffusion constants.
where b_m is the hydrodynamic length of the monomer unit and d_h its thickness, A_m is the length of the statistical chain element, i.e., the length of the average number of monomer units after which a kink in the molecular chain occurs, Z is the degree of polymerization, k is Boltzmann's constant, N is Avogadro's number, M_0 is the molecular weight of the base unit and η_0 is the viscosity of the solvent.

The length A_m of the statistical chain element is determined by the two definitions (ref. 91)

$$L = Z\, b_m = K A_m, \quad \bar{R}^2 = K A_m^2$$

yielding

$$A_m = \bar{R}^2 / L \tag{84}$$

where L is the so-called hydrodynamic length, i.e., the fully extended length of the chain, as can be obtained without distortion of valence angles or atomic distances and $\bar{R}^2$ is the mean-square end-to-end distance of the chain.

For very high molecular weights the first two terms in the denominator of equation (77) can be neglected and $[\eta]$ becomes proportional to $Z^{\frac{1}{2}}$. For rigid chains of low molecular weight, for which $A_m = b_m Z$, $[\eta]$ becomes proportional to Z^2.

In the treatment of Debye and Bueche (92) the coiled polymer molecule is replaced by a porous sphere of radius R_s uniformly filled with resisting points equal to the number of monomer units in the molecule. The degree of porosity of this sphere determines the hydrodynamic interaction. The flow of solvent through the aggregate of beads is treated by a modification of the Navier-Stokes equations leading to the results

$$[\eta] = \frac{4\pi N}{3} \frac{R_s^3}{M} \Phi(\sigma) \tag{85}$$

$$[s] = \frac{s_0 \eta_0}{1 - V\varrho} = \frac{M}{6\pi R_s N} \frac{1}{\psi(\sigma)} \tag{86}$$

$$D = \frac{kT}{6\pi \eta_0 R_s} \frac{1}{\psi(\sigma)} \tag{87}$$

where $\Phi(\sigma)$ and $\psi(\sigma)$ are volume factors dependent on the "shielding ratio", σ. The latter is defined by the equations

$$\sigma = \frac{R_s}{K^{\frac{1}{2}}}, \qquad K = \frac{(2R_s)^3}{36 Z f}$$

where k is the permeability of the sphere, f is the frictional constant per monomer unit and Z is the degree of polymerization. R_s is related to the dimensions of the coil by the expression

$$2R_s = 1.054 R$$

where R is the end-to-end distance.

If the swarm is very open, Staudinger's law is obtained as one limit. If, in the other limit, the swarm becomes impenetrable, the viscosity becomes proportional to $M^{\frac{1}{2}}$.

In its initial physical assumptions the Kirkwood-Riseman theory (93) is more rigorous. The model used is that of hampered flow through beads arranged as in a random coil. The hydrodynamic interaction between the different parts of the molecule is calculated directly on the basis of the classical hydrodynamic equations of motion. The relations obtained are

$$[\eta] = \frac{N \xi b^2 Z}{3600 \eta_0 M_0} F(\lambda_0 Z^{\frac{1}{2}}) \tag{88}$$

where

$$\lambda_0 = \xi/(6\pi^3)^{\frac{1}{2}} \eta_0 b \tag{89}$$

and

$$F(x) = F(\lambda_0 Z^{\frac{1}{2}}) = 6/\pi^2 \sum_{k=1}^{\infty} \frac{1}{k^2} \frac{1}{1 + x/k^{\frac{1}{2}}} \tag{90}$$

$$Z = M/M_0.$$

The independent molecular parameters are Z the degree of polymerization, b the effective bend length, i.e., the length of the statistically independent units of the chain, ξ the frictional coefficient of the single beads and η_0 the viscosity of the medium. From equations (88) to (90) it follows that as Z varies from 0 to ∞ the dependence of $[\eta]$ on M varies from M to $M^{\frac{1}{2}}$.

The frictional resistance associated with the translational motion of the flexible molecule is given by

$$f_T = \frac{Z \xi}{1 + \frac{8}{3} Z^{\frac{1}{2}} \lambda_0} \tag{91}$$

whence the sedimentation and diffusion constants are obtained as

$$D = \frac{kT}{Z \xi} [1 + \tfrac{8}{3} \lambda_0 Z^{\frac{1}{2}}] \tag{92}$$

$$s = \frac{M_0}{N \xi} (1 - V \varrho) [1 + \tfrac{8}{3} \lambda_0 Z^{\frac{1}{2}}]. \tag{93}$$

The Debye-Bueche and Kirkwood Riseman theories emphasize the degree of coil permeability as a function of molecular weight. In a more recent theory Flory and

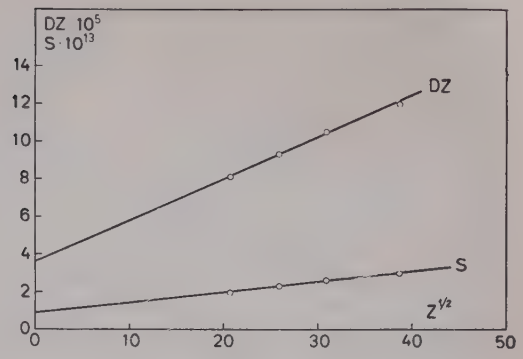

Fig. 25. Plots of DZ and s against $Z^{\frac{1}{2}}$ for ethyl hydroxyethyl cellulose in water. D, s and Z are respectively the diffusion and sedimentation constants and the degree of polymerization.

Fox (94, 95) concentrate on the change of the coil dimensions with M. They postulate that the intrinsic viscosity of a polymer in solution should be proportional to the ratio of the volume occupied by the molecule to the molecular weight. As a measure of the volume of the molecule they use the cube of the root-mean-square end-to-end distance and they show that as the combined result of long range interactions between segments and of segment-solvent interaction, the molecular dimensions will be increased by a factor α. The intrinsic viscosity is thus given by the following relations

$$[\eta] = K M^{\frac{1}{2}} \alpha^3, \qquad \alpha = (\bar{R}^2/\bar{R}_0^2)^{\frac{1}{2}} \tag{94}$$

$$K = \Phi (\bar{R}_0^2/M)^{3/2} \tag{95}$$

$$C_T = 2 \psi_1 C_M (1 - \theta/T) = (\alpha^5 - \alpha^3)/M^{\frac{1}{2}} \tag{96}$$

$$[\eta]^{\frac{2}{3}}/M^{\frac{1}{3}} = K^{\frac{2}{3}} + K^{5/3} C_T M/[\eta] \tag{97}$$

where K is a constant characteristic of the polymer and the temperature, $(\bar{R}_0^2)^{\frac{1}{2}}$ is the root-mean-square end-to-end distance in the absence of perturbation due to the solvent and long range interaction; Φ is a hydrodynamic constant (for sufficiently high molecular weights) which should be the same for all polymers irrespective of solvent, T is the absolute temperature, ψ_1 and C_M are thermodynamic constants, α is the ratio of the actual root-mean-square end-to-end distance to the unperturbed value, θ is the critical miscibility temperature for the polymer-solvent (of infinite molecular weight) system.

By an analogous argument Mandelkern and Flory (96) show that the frictional coefficient may be represented by the relation

$$f_0/\eta_0 = P (\bar{R}^2)^{\frac{1}{2}} = P \left(\frac{\bar{R}_0^2}{M}\right)^{\frac{1}{2}} M^{\frac{1}{2}} \alpha \tag{98}$$

where P is a "universal" constant analogous to Φ of the viscosity theory and η_0 is the viscosity of the solvent. By combining equations (20), (94), (95) and (98) the following relation between the sedimentation constant and the intrinsic viscosity is obtained:

$$s_0 [\eta]^{\frac{1}{3}}/M^{\frac{2}{3}} = \Phi^{\frac{1}{3}} P^{-1} N^{-1} (1 - V\varrho)/\eta_0. \tag{99}$$

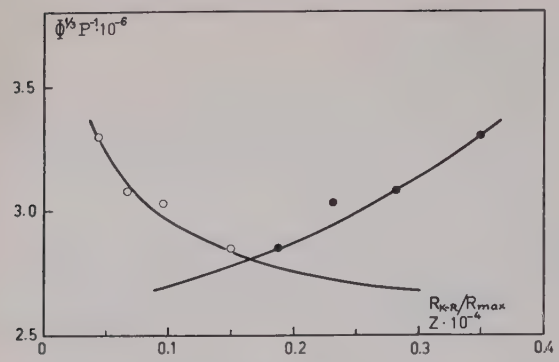

Fig. 26. Variation of $\Phi^{\frac{1}{3}} P^{-1}$ with extension ratio R_{K-R}/R_{max} (filled circles) and degree of polymerization (open circles).

The corresponding equation for the relation between the diffusion constant and the molecular weight is

$$D_0 \eta_0 (M[\eta])^{\frac{1}{3}} = k T P^{-1} \Phi^{\frac{1}{3}} \tag{100}$$

where k is the Boltzmann constant and T the absolute temperature. The theory predicts that for a series of homologous polymer fractions in a given solvent, the left hand member of equations 99 and 100 should be independent of M.

We turn now to an evaluation of the present experimental data in the light of the above theories. According to the theory of Kuhn and Kuhn the dependence of s and D on Z is given by equations 78 and 79. By introducing the experimentally observed values of a_1, b_1, a_2, b_2 into equations (80) to (83) the parameters A_m and d_h can be determined since all the other parameters are known from the experimental conditions. In Fig. 25, s_0 and DZ are plotted against $Z^{\frac{1}{2}}$. From the slope and intercept of these lines and using the values $M_0 = 210$, $b_m = 5.15 \times 10^{-8}$ cm, $V = 0.7$ it follows that

$$A_m = 120 \text{ Å and } d_h = 0.1 \text{ Å}.$$

The sedimentation and diffusion data lead to exactly the same result. Knowing A_m and d_h the intrinsic viscosities were calculated for the four fractions. The results given in Table 19 are in all cases about 50 per cent lower than the experimentally observed values. The value of A_m seems to be of the right order of magnitude and corresponds on the average to about 23 glucose rests per link. The molecule is thus appreciably uncoiled. For cellulose acetate in acetone and methyl cellulose in water,

Table 19. Intrinsic viscosities and molecular dimensions of ethyl hydroxyethyl cellulose as calculated from the theories of Debye-Bueche (D-B), Kirkwood-Riseman (K-R) and Kuhn-Kuhn (K-K).

Fraction No.	$[\eta]_{20}$ obs. dl/g	$[\eta]_{20}$ D-B dl/g	R_s(Å) D-B	R(Å) D-B	$[\eta]_{20}$ K-K dl/g	R(Å) K-K	$[\eta]_{20}$ K-R dl/g	R(Å) K-R	R_{K-R}/R_{max}
12	9.4	3.86	396	750	4.36	960	10.8	1430	0.19
7	7.0	2.70	307	580	3.17	770	7.48	1140	0.23
5	5.0	1.94	244	460	2.24	640	5.55	960	0.28
3	3.7	1.10	176	330	1.73	514	3.80	770	0.35

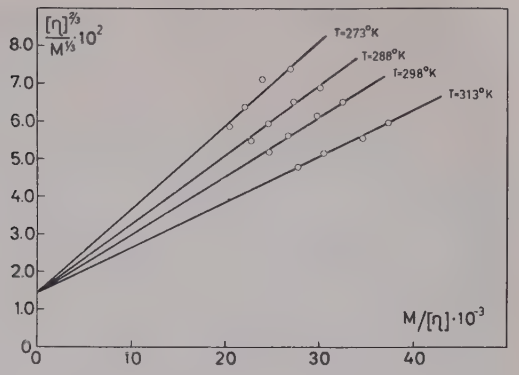

Fig. 27. Plots of $[\eta]^{\frac{2}{3}}/M^{\frac{1}{3}}$ versus $M/[\eta]$ for fractions of ethyl hydroxyethyl cellulose in water at various temperatures. The intercept corresponds to $K = 18 \times 10^{-4}$ (see equation (97)).

values of 110 Å and 50 Å respectively have been reported (88). On the other hand the value of d_h is somewhat unrealistic. For the two systems just mentioned the values are respectively 11 Å and 8 Å. This may indicate that the resistance of the coil to translational and rotational motion does not depend on the frictional resistance of the monomer in the manner suggested by the equations.

For the determination of R_s and σ in the Debye-Bueche theory any of the equations (85), (86) and (87) together with its logarithmic derivative

$$\frac{d \log [\eta]}{d \log M} = \varepsilon_1 = -1 + \frac{1}{2}\frac{d \log \phi}{d \log \sigma} + \left(3 - \frac{1}{2}\frac{d \log \phi}{d \log \sigma}\right)\frac{d \log 2R_s}{d \log M} \tag{101}$$

$$\varepsilon = \frac{d \log s}{d \log M} = 1 - \varepsilon_2 = \left(1 - \frac{1}{2}\frac{d \log \psi}{d \log \sigma}\right)\left(1 - \frac{d \log 2R_s}{d \log M}\right) \tag{102}$$

$$\frac{d \log D}{d \log M} = -\varepsilon_2 \tag{103}$$

may be used (91).

From the value of ε_1 and ε_2 as determined from the experimentally observed dependence of $[\eta]$ and s on M (see equations (69) and (75)) the values of the shielding ratio and volume factor were found by interpolation in tables given by the authors. The results are

$$[\eta] = K_\eta M^{\varepsilon_1};\ \varepsilon_1 = 0.8,\ \sigma = 3.6;\ \Phi(\sigma) = 0.74,$$
$$s = K_s M^{\varepsilon};\ \varepsilon_2 = 0.64;\ \sigma = 3.4;\ \psi(\sigma) = 0.65.$$

Values of R_s were then calculated by substitution in equation (86). Finally from a knowledge of R_s and $\Phi(\sigma)$ values of $[\eta]$ were calculated from equation (85). The results shown in Table 19 are about 50 per cent lower than the observed values.

The parameters ξ and λ_0 in the Kirkwood-Riseman theory were evaluated in accordance with equation 93 from the slope and intercept of the s against $Z^{\frac{1}{2}}$ plot. The effective bond length b was then calculated by substitution in equation (89). The values obtained are

$$b = 37 \text{ Å};\ \xi = 11.2 \times 10^{-10} \text{ g/sec.};\ \lambda_0 = 22.9 \times 10^{-3}.$$

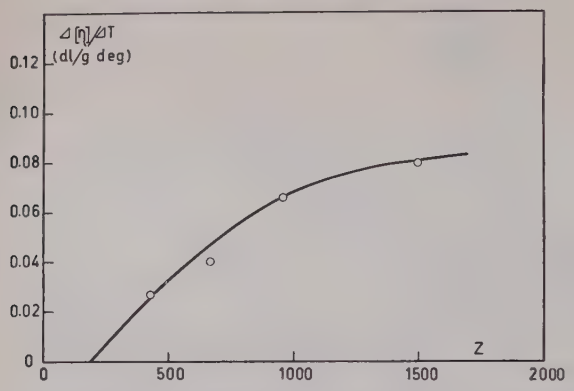

Fig. 28. Variation of temperature coefficient of intrinsic viscosity with degree of polymerization for ethyl hydroxyethyl cellulose in water.

For cellulose nitrate in acetone (97) and polystyrene in toluene (98) values of b of 35 Å and 8.6 Å respectively have been reported. The high value of b obtained here again indicates that the molecules are highly extended.

Intrinsic viscosities calculated from equation (88), using values of $F(\lambda_0 Z^{\frac{1}{2}})$ tabulated by Kirkwood and Riseman, are given in Table 19. For all fractions there is reasonable agreement with the observed values.

Molecular dimensions calculated from these three theories are given in Table 19. From the foregoing it is clear that the K–R values are to be considered the most reliable. It is to be expected that estimates made on the basis of various theories will differ, because of the different assumptions made. The fundamental relationships of the Debye-Bueche and Kirkwood-Riseman theories are essentially identical except for numerical factors (cf. e.g. ref. 99). Since in all the above calculations average molecular parameters have been used, the dimensions obtained are also average values.

According to equation (99) the quantity $s[\eta]^{\frac{1}{3}}/M^{\frac{2}{3}}$ evaluated for a series of polymer fractions should be constant independent of the nature of the polymer, the solvent and the temperature. The values given in Table 20 show a tendency to decrease with increasing molecular weight. Values of $\Phi^{\frac{1}{3}} P^{-1}$ calculated according to equations 99 and 100 also exhibit the same trend. This decrease is larger than can be accounted for either by the observed variations in the factor $(1 - V\varrho)/\eta_0 N$ (see Table 20), by the probable error of the measurements or by the polydispersity of the fractions. The effect of the latter would be to cause an increase in the absolute value of $\Phi^{\frac{1}{3}} P^{-1}$ for each fraction (100). For other linear polymer systems values of $\Phi^{\frac{1}{3}} P^{-1}$ range from 2.3 to 2.7 $\times 10^6$. Mandelkern *et al.* (101) have summarized the

Table 20. Values of $\Phi^{1/3} P^{-1}$ for ethyl hydroxyethyl cellulose in water.

Fraction No.	$\frac{s[\eta]^{1/3}}{M^{2/3}} \times 10^{17}$	$\frac{1 - V\varrho}{\eta_0 N} \times 10^{21}$	$(\Phi^{1/3} P^{-1})_{sed} \times 10^6$	$[\Phi^{1/3} P^{-1})_{diff} \times 10^6$
12	14.1	4.888	2.90	2.80
7	14.7	4.921	3.01	3.05
5	14.7	4.799	3.08	3.08
3	15.2	4.619	3.30	3.29

work of many authors and report an average of 2.5×10^6. In Fig. 26, $\Phi^{\frac{1}{3}} P^{-1}$ is plotted against the degree of polymerization, Z. From the shape of the curve it appears that a limiting value of $2.5–2.7 \times 10^6$ would be reached at a value of Z somewhat greater than 2500, or a molecular weight of about 500,000.

The cause of this behavior probably lies in the high extension of the cellulose molecule at low and moderate degrees of polymerization. The Flory-Fox theory is only valid for those polymer systems in which the extension of the molecules is so low that their spatial distribution is spherically symmetric. There must therefore be a considerable degree of solvent immobilization. As pointed out by Flory (102), such a condition will only hold if the polymer molecules are irregularly coiled to an extent such that the root-mean-square end-to-end distance $(\bar{R}^2)^{\frac{1}{2}}$ does not exceed one-tenth of $(\bar{R}^2)^{\frac{1}{2}}_{\max}$, the length of the molecule at full extension. For vinyl and similar polymers this is normally true down to molecular weights of $2–4 \times 10^4$. In Table 19 the values of the extension ratios $(\bar{R}^2)^{\frac{1}{2}}/(\bar{R}^2)^{\frac{1}{2}}_{\max}$ are given. $(\bar{R}^2)^{\frac{1}{2}}_{\max}$ is obtained as the product of the degree of polymerization and the length of the glucose residue (5.15 Å). The values of $(\bar{R}^2)^{\frac{1}{2}}$ are those calculated from the Kirkwood-Riseman theory. The extension ratios are rather high (see also Table 10) and the increase in $\Phi^{\frac{1}{3}} P^{-1}$ is paralleled by an increase in the extension ratio. Furthermore, as shown in Fig. 26, $\Phi^{\frac{1}{3}} P^{-1}$ shows a tendency to approach the accepted value at extension ratios less than 0.1.

A similar situation is found when the constant Φ is calculated from equations (94) and (95) using M_{ww} and $(\bar{R}^2)^{\frac{1}{2}}$ from the Kirkwood-Riseman theory. It is found to have values ranging from 0.74×10^{21} at low M to 0.96×10^{21} at high M in contrast to 2.1×10^{21} for Gaussian coil polymers. These results are quite in keeping with the previous conclusions as to the configuration of the ethyl hydroxyethyl cellulose molecule in solution. All the evidence indicates that, as with other cellulose derivatives (103), the molecules here are linear with a very open and almost free-draining configuration.

It is of interest to consider the effects of interactions between the glucose residues in the chain. For an unbranched chain the mean-square end-to-end distance is related to the degree of polymerization by the equation (refs. 104, 105)

$$b^2 Z = \bar{R}^2 = Z l^2 \left(\frac{1+\cos\theta}{1-\cos\theta}\right)\left(\frac{1+\overline{\cos\varphi}}{1-\overline{\cos\varphi}}\right) \tag{104}$$

where l is the bond length, equal to 5.15 Å, θ is the supplement of the valence angle—equal to 70° for cellulose and its derivatives, and $\overline{\cos\varphi}$ is the mean value of the cosine of the angle between successive bond planes. Using the value of b calculated from the Kirkwood-Riseman theory, $\overline{\cos\varphi}$ is found to be 0.924. Since $\overline{\cos\varphi}$ is zero if there is free rotation about the bonds it is evident that the chain is very greatly extended over the free rotation size. This effect is responsible for the lack of flexibility in cellulose and its derivatives. In the present case it is probable that the hindrance to rotation about the oxygen linking the glucose units is somewhat enhanced by the side groups.

Finally it is possible to relate the activation energy of viscous flow to the parameters α and K in the Flory-Fox viscosity theory by the equation (ref. 106)

$$\frac{d \ln [\eta]}{d(1/T)} = 3\frac{d \ln \alpha}{d(1/T)} + \frac{d \ln K}{d(1/T)}. \tag{105}$$

It follows that the temperature coefficient of viscosity is due partly to the swelling of the molecules, $d \ln \alpha / d(1/T)$, and partly to internal modifications in the structure of the molecule ($d \ln K / d(1/T)$) caused, for example, by steric hindrance in the rotation of the segments.

The Flory theory cannot be used for the quantitative calculation of molecular dimensions in the range of molecular weights studied here; it does, however, allow certain qualitative conclusions to be drawn as to the relative importance of α and K in equation (105). According to equation (97), K may be ascertained from the intercept of a plot of $[\eta]^{\frac{1}{3}}/M^{\frac{1}{3}}$ against $M/[\eta]$. As seen in Fig. 27, a long and uncertain extrapolation is involved but within the limits of the experimental error K is independent of temperature. This is in sharp contrast to the behavior of other cellulose derivatives (107) and indicates that in the present system the change of viscosity with temperature is largely the result of swelling effects which undoubtedly arise from the increased molecular hydration at low temperatures.

Support for this point of view is also found in the variation of intrinsic viscosity with temperature (see Fig. 7). The decrease in viscosity with increase in temperature implies a corresponding change in solubility. This is, of course, contrary to normal solubility behavior and must mean that an addition compound is formed with water which is less stable at higher temperatures. Thus it is not ethyl hydroxyethyl cellulose itself which is soluble in water but rather its reaction product with water.

In Fig. 28 the temperature coefficient of viscosity is given as a function of the degree of polymerization, Z. The temperature coefficient vanishes at a degree of polymerization of about 200, indicating that at lower values the molecule is so highly extended that the swelling effects cease to be of importance. From this and the previously discussed behavior of the quotient $\Phi^{\frac{1}{3}} P^{-1}$, it is expected that the relations between the molecular weight and the various frictional constants, $[\eta]$, s and D should be valid for degrees of polymerization between 200 and 2500. Beyond these limits changes in the form of the molecule should be reflected in the value of the molecular weight exponent.

Summary

The non-ionic water soluble cellulose ether ethyl hydroxyethyl cellulose was fractionated by extraction with acetone-water solutions of varying acetone content. The method gave fractionation both with respect to degree of polymerization and chemical composition. The later effect was, however, confined to the species of lowest degree of polymerization. Of twelve fractions obtained four were selected for the characterization of the polymer.

Viscosity measurements were made at four temperatures in the range 0–40°C. The influence of surface tension and velocity gradient was investigated and found to be negligible. The solutions showed high intrinsic viscosities and high negative temperature coefficients of viscosity.

Number average molecular weights were determined from osmotic pressure measurements using a Fuoss-Mead osmometer with interferometric registration of height differences. Values obtained ranged from 50,000–180,000.

In ultracentrifugation studies the sedimentation curves showed a well defined fairly symmetrical peak. The sedimentation coefficients were extrapolated linearly

to infinite dilution in accordance with the relation

$$s = s_0 (1 + k c + k' c^2).$$

The values of the sedimentation constants lay in the range 2–3 Svedberg units.

Diffusion coefficients, measured by the free boundary technique with the aid of the Lamm scale method, showed a linear concentration dependence and were extrapolated to infinite dilution graphically. The diffusion constants thus obtained lay in the range $0.8–1.9 \times 10^{-7}$ cm^2/sec.

Molecular weights computed from the Svedberg equation ranged from 90,000–300,000. Frictional coefficients, axial ratios and molecular dimensions were calculated from the sedimentation–diffusion data. The samples were characterized by high axial ratios and high frictional coefficients.

Sedimentation equilibrium measurements permitted the estimation of weight average molecular weights. The results showed good agreement with those from sedimentation–diffusion.

Angular dependence light scattering measurements gave molecular weights which were 80–100 per cent higher than those from sedimentation–diffusion and sedimentation equilibrium. The discrepancy is shown to originate in a small quantity of large particulate matter present in the solutions despite all efforts at optical clarification. The aggregated material is presumed to arise from the biological structure elements of the original cellulosic material.

Relations between molecular weight and intrinsic viscosity, sedimentation and diffusion constants are given.

The interpretation of the data in terms of current hydrodynamic theories leads to the conclusion that the molecules are hydrated linear chains coiled in an approximately free draining fashion.

Finally, the high temperature coefficient of viscosity is shown to be due to changes in the stability of the addition compound formed between polymer and solvent.

REFERENCES

1. Ott, E., Cellulose and Cellulose Derivatives. Interscience, N.Y. (1955).
2. Timell, T., Studies on Cellulose Reactions. Dissertation, Stockholm (1950).
3. Jullander, I., Svensk Kem. Tidskr. *65*, 223 (1953); Chimie et Industrie *71*, 228 (1954).
4. Signer, R. and Liechti, J., Helv. chim. Acta *21*, 530 (1938).
5. Signer, R. and Tavel, P., ibid. *21*, 535 (1938).
6. Polson, A., Koll.-Z. *83*, 172 (1938).
7. Staudinger, H. and Reinecke, F., Ann. *47*, 535 (1938).
8. Jullander, I., Svensk Papperstidn. *55*, 197 (1952).
7. Staudinger, H. and Reinecke, F., Ann. *47*, 535 (1938).
8. Jullander, I., Svensk Papperstidn. *55*, 197 (1952).
9. Heyman, E., Trans. Faraday Soc. *31*, 846 (1935).
10. Heyman, E., Bleakley, H. G., and Docking, A. R., J. Phy. Chem. *42*, 353 (1938).
11. Docking, A. R., Australian Chem. Inst. J. and Proc. 400 (1939).
12. Sönnerskog, S., Some Ethers of Cellulose and Starch. Dissertation, Stockholms Högskola, Stockholm (1952).
13. Jullander, I., Svensk Papperstidn. *56*, 443 (1953).
14. Lemieux, R. V. and Purves, C. B., Can. J. Research B *25*, 485 (1947).
15. Morgan, P. W., Ind. Eng. Chem., Anal. Ed., *18*, 500 (1946).
16. Pals, D. T. and Hermans, J. J., Rec. Trav. Chim. *71*, 441 (1952).
17. Masson, C. R. and Melville, H. W., J. Polymer Sci. *4*, 338 (1949).
18. Schurz, J. and Immergut, E. H., J. Polymer Sci. *9*, 279 (1952).

19. Meissner, W., Chem. Rev. Fett-Harz-Ind. *19*, 30, 44 (1912).
20. Kroepelin, H., Koll.-Z. *47*, 294 (1929).
21. Jones, G. and Fornwalt, H. J., J. Am. Chem. Soc. *60*, 1683 (1938).
22. Pals, D. T. and Hermans, J. J., Rec. Trav. Chim. *71*, 441, 458 (1952).
23. Philippoff, W., Viskosität der Kolloide. Steinkopff, Dresden and Leipzig 1942. Pp. 56–57.
24. Flory, P. J., J. Chem. Phys. *10*, 51 (1942).
25. Huggins, M. L., J. Phys. Chem. *46*, 151 (1946).
26. Flory, P. J. and Krigbaum, W. R., J. Chem. Phys. *18*, 1806 (1950).
27. Wall, F. T. and Hiller, L. A., Ann. Rev. of Physical Chem. *5*, 274 (1954).
28. Jacobsson, G., Acta Chem. Scand. *7*, 582 (1953).
29. Claesson, S. and Jacobsson, G., ibid. *8*, 1835 (1954).
30. Jacobsson, G., ibid. *8*, 1843 (1954).
31. Fuoss, R. M. and Mead, D. J., J. Phys. Chem. *48*, 59 (1944).
32. Gee, G., Trans. Faraday Soc. *36*, 1162 (1940).
33. Montonna, R. E. and Jilk, W. T., J. Phys. Chem. *45*, 1374 (1941).
34. Lang, H., Kolloid-Z. *122*, 165 (1951).
35. Svedberg, T. and Pedersen, K. O., The Ultracentrifuge. Oxford 1940. (Die Ultrazentrifuge. Dresden und Leipzig 1940.)
36. Lamm, O., Nova Acta Reg. Soc. Scient. Upsaliensis *IV*, 10, No. 6 (1937).
37. Gralén, N., Sedimentation and Diffusion Measurements on Cellulose and Cellulose Derivatives. Inaugural Dissertation, Uppsala 1944.
38. Jullander, I., Ark. Kemi, Min. och Geol. *21A*, No. 8 (1945).
39. Kermack, W. O., Mc Kendrick, A. G., and Ponder, E., Proc. Roy. Soc. Edinburgh *49*, 193 (1928).
40. Burgers, J. M., Proc. Acad. Sci. Amsterdam *44*, 1045, 1177; *45*, 9, 136 (1942).
41. Signer, R. and Gross, H., Helv. chim. Acta *17*, 59, 335, 726 (1934).
42. Newman, S. and Eirich, F., J. Colloid Sc. *5*, 541 (1950).
43. Newman, S., Loeb, L., and Conrad, C. M., J. Polymer Sc. *10*, 463 (1953).
44. Lauffer, M., J. Amer. Chem. Soc. *66*, 1195 (1944).
45. Powell, R. and Eyring, H., Advances in Colloid Science, Vol. 1, p. 183.
46. Signer, R. and Egli, H., Receuil *69*, 45 (1950).
47. Wiener, O., Ann. der Physik und Chemie *49*, 105 (1893).
48. Beckmann, D. O. and Rosenberg, J. L., Ann. N.Y. Acad. Sci. *46*, 329 (1945).
49. Claesson, S., Nature *158*, 834 (1946).
50. Gosting, L. R. and Morris, M. S., J. Am. Chem. Soc. *71*, 1998 (1949).
51. Herzog, R. O., Illig, R., and Kudar, H., Z. physik. Chem. *A 167*, 329 (1933).
52. Williams, J. W., Saunders, W. M., and Cicirelli, J. S., J. Phys. Chem. *58*, 778 (1954).
53. Schulz, G. V., Z. physik. Chem. *A 193*, 168 (1944).
54. Wales, M., Bender, M. M., Williams, J. W., and Ewart, R. H., J. Chem. Phys. *14*, 353 (1946).
55. Wales, M., J. Phys. and Colloid Chem. *52*, 235 (1948).
56. Doty, P. and Edsall, J. T., Advances in Protein Chem. *6*, 79 (1951).
57. Oster, G., Chem. Revs. *43*, 319 (1948). Progr. Biophys. and Biophys. Chem. *1*, 73 (1950).
58. Mark, H., Frontiers in Chem. *5*, 121 (1946).
59. Sadron, C., J. Polymer Sci. *12*, 69 (1954).
60. Zernike, F., L'opalescence critique. Thesis, Amsterdam 1915; Arch. Neerland. Sci. III A 4, 74 (1918).
61. Debye, P., J. Applied Phys. *15*, 338, 1944; J. Phys. and Colloid Chem. *51*, 18 (1947).
62. Zimm, B. H., J. Chem. Phys. *16*, 1093 (1948).
63. Lord Rayleigh, Proc. Roy. Soc. London *A 84*, 25 (1911).
64. Gans, R., Ann. Physik *76*, 29 (1925).
65. Neugebauer, T., Ann. Physik *42*, 509 (1943).
66. Zimm, B. H., Stein, R. S., and Doty, P., Polymer Bull. *1*, 90 (1945).
67. Zimm, B. H., J. Chem. Phys. *16*, 1099 (1948).
68. Benoit, H., Holtzer, A. M., and Doty, P., J. Phys. Chem. *58*, 635 (1954).
69. Brice, B. A., Halwer, M., and Speiser, R., J. Opt. Soc. Amer. *40*, 768 (1950).
70. Hermans, J. J. and Levinson, S., J. Opt. Soc. Amer. *41*, 460 (1951).
71. Alexander, P. and Stacey, K., Paper read at the Congress on Macromolecular Chemistry, Milan 1954.
72. Frank, H. P. and Mark, H. F., Report on Molecular weight measurements of standard polystyrene samples. J. Polymer Sci. *17*, 1 (1955).

73. Williams, J. W., Saunders, W., and Cicirelli, J., J. Phys. Chem. *58*, 774 (1954).
74. Lansing, W. D. and Kraemer, E. O., J. Am. Chem. Soc. *57*, 1369 (1935).
75. Williams, J. W., J. Polymer Sci. *12*, 351 (1954).
76. Eriksson, A. F., Acta Chem. Scand. In Press.
77. Doty, P., Wagner, H., and Singer, S., J. Phys. and Coll. Chem. *51*, 32 (1947).
78. Hess, K., Holzforschung *9*, 65 (1955).
79. Dürig, G., and Banderet, A., Helv. chim. Acta *33*, 1106 (1950).
80. Ott, E. and Elliott, J. H., Makromol. chim. 18/19, 352 (1955).
81. Höppler, F., Kolloid-Z. *98*, 348 (1942).
82. Singer, S., J. Polymer Sci. *1*, 445 (1946).
83. Schulz, G. V., Cantow, H., and Meyerhoff, G., J. Polymer Sci. *10*, 79 (1953).
84. Staudinger, H., Die hochmolekularen organischen Verbindungen, J. Springer, Berlin.
85. Flory, P. J., J. Am. Chem. Soc. *65*, 372 (1943).
86. Flory, P. J., Principles of Polymer Chemistry. Cornell Univ. Press. (1953).
87. Kuhn, W. and Kuhn, H., Helv. chim. Acta 1394 (1943).
88. Kuhn H., and Kuhn, W., Helv. chim. Acta *30*, 1233 (1947); J. Chem. Phys. *16*, 838 (1948); J. Polymer Sci. *5*, 519 (1950); ibid. *9*, 1 (1952); J. Colloid Sci. *5*, 331 (1950).
89. Kuhn, H., Kuhn, W., and Silverberg, A., J. Polymer Sci. *10*, 79 (1953).
90. Kuhn, H., Moning, F., and Kuhn, W., Helv. chim. Acta *36*, 731 (1953).
91. Peterlin, A., J. Colloid Sci. *10*, 587 (1955).
92. Debye, P. and Bueche, A. M., J. Chem. Phys. *16*, 573 (1948).
93. Kirkwood, J. G. and Riseman, J., J. Chem. Phys. *16*, 565 (1948).
94. Flory, P. J. and Fox, T. G., J. Polymer Sci. *5*, 745 (1950).
95. Flory, P. J. and Fox, T. G., J. Am. Chem. Soc. *73*, 1904 (1951); ibid. *73*, 1915 (1951).
96. Mandelkern, L. and Flory, P. J., J. Chem. Phys. *20*, 212 (1952).
97. Holtzer, A., Benoit, H., and Doty, P., J. Phys. Chem. *58*, 624 (1954).
98. Newman, S., Riseman, J., and Eirich, F., Proc. Int. Colloq. Macromols. Amsterdam (1949).
99. Schulz, G. V., Cantow, H. J., and Meyerhoff, G., J. Polymer Sci. *10*, 84 (1953).
100. Gouinlock, E. V., Flory, P. J., and Scheraga, H. A., J. Polymer Sci. *14*, 383 (1955).
101. Mandelkern, L., Krigbaum, W. R., Scheraga, H. A., and Flory, P. J., J. Chem. Phys. *20*, 1392 (1952).
102. Newman, S., Krigbaum, W. R., Langier, C., and Flory, P. J., J. Polymer Sci. *14*, 451 (1954).
103. Doty, P., Schneider, N. S., and Holtzer, A., J. Am. Chem. Soc. *75*, 754 (1953).
104. Taylor, W. J., J. Chem. Phys., *16*, 257 (1948).
105. Benoit, H., J. Chim. Phys. *44*, 18 (1947); J. Polymer Sci. *3*, 376 (1948).
106. Dieu, H., J. Polymer Sci. *12*, 417 (1954).
107. Mandelkern, L. and Flory, P. J., J. Am. Chem. Soc. *74*, 2517 (1952).

Tryckt den 7 maj 1956

Uppsala 1956. Almqvist & Wiksells Boktryckeri AB